Woods, A.J., Duncan, A.J., Tseng, Y.-T., Gavrilov, A.N., Perry, M.A., McCauley, R.D. (2005) "Epibenthic Scattering Project (ESP): Report on Experimental Deployments and Outcomes for Toolkit", Coastal Zone CRC Milestone Report Number CA6.03.2, CMST Report 2005-65, Curtin University of Technology, November 2005.

Coastal CRC
Coastal Water Habitat Mapping project
CA – Shallow Water Assessment Technologies
Epibenthic Scattering Project

CRC Milestone Report Number CA6.03 – Part 2
(ESP Project Milestone 6)

"Epibenthic Scattering Project (ESP): Report on Experimental Deployments and Outcomes for Toolkit"

28 November 2005

Prepared by Andrew Woods
With support from Alec Duncan, Yao-Ting Tseng, Alexander Gavrilov, Mal Perry, and Rob McCauley.

Table of Contents

Introduction

The aim of this project has been to develop innovative acoustic techniques as a tool for detection, classification, and mapping of marine vegetation on the seafloor. To achieve this aim it was recognised that a thorough understanding of the acoustic backscatter process from epibenthos would be required and this project (ESP – Epibenthic Scattering Project) has focused on obtaining this understanding.

This report outlines the equipment that has been developed for the project, describes three field deployments of the ESP system in Cockburn Sound for data collection, and summarises the data processing that has been conducted to date.

One of the unique features of this project has been the process of collecting coincident optical and acoustic data, which is taking digital still photographs of the same piece of sea floor as the acoustic systems samples at the same time. The purpose of doing this is that the acoustic returns can be compared with photographs for the same place and time so that we know exactly what the sonars were observing. The reciprocal optical-acoustical system is capable of observing different seabed habitat types as well as detecting fish or unnatural objects on or near the seafloor. Moreover, the digital still photographs were taken by a stereo-pair of two cameras, which allowed us to estimate the canopy height of marine vegetation.

Equipment

The equipment used for the project consisted of a mixture of off-the shelf systems combined with a range of custom designed electronics and supported with software specially developed for the system.

The overall block diagram of the ESP system is shown in Appendix 1.

The overall ESP system consisted of two parts, the wet-end and the dry-end.

The three main data collection sensors used for the ESP system are:

1. Simrad EQ60 dual-frequency single-beam echosounder,
2. TAPS (Tracor Acoustic Profiling System) six frequency single-beam echosounder, and
3. Curtin underwater stereoscopic digital still camera.

Other sensors include a differential GPS (for logging location) and a tri-axial accelerometer in the camera housing (for measuring orientation of the camera).

The wet-end of the ESP system is shown in Figure 1 and consists of the EQ60 transducer, the TAPS echosounder, the stereoscopic digital still camera, and a light source all mounted in a stainless steel frame.

The wet-end of the ESP system contains 8 individual echo sounder transducers, 2 in the Simrad EQ60 transducer head, and 6 in the TAPS (Tracor Acoustic Profiling System) head. Both sonars were aimed at the same area of the seabed.

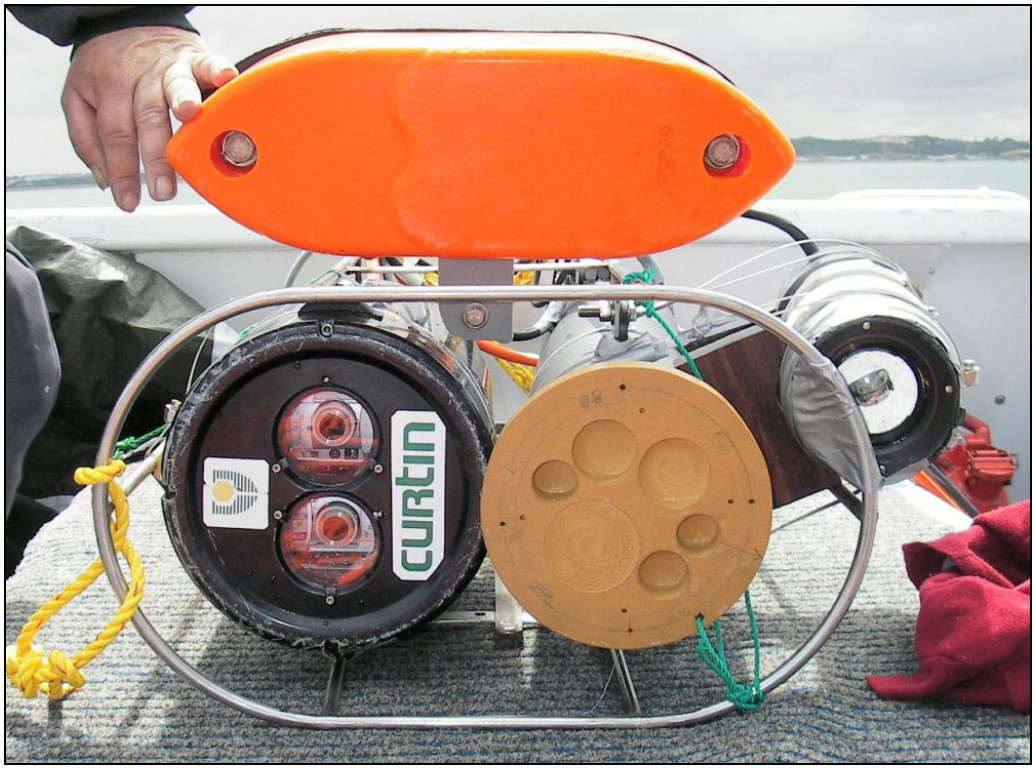

Figure 1: Wet end of the ESP system as used in the third field trial.
[Top: EQ60 transducer, left: digital still stereoscopic camera,
middle: TAPs fitted with attenuating mask, and far right: light source (strobe).]

The internals of the underwater stereoscopic digital still camera system are shown in Figure 2. The camera consists of a pair of Canon 5-megapixel digital still cameras which have been modified to fire synchronously with each other (generally within 8ms of each other). Mounted in the same housing as the cameras is the wet-end microcontroller (WEM) which acts to (a) communicate with the surface computer via a serial connection (receives commands and transmit data), (b) provides control signals for the cameras, (c) provides a channel select signal for the video multiplexer, and (d) reads the triaxial accelerometer (inclinometer). Three other electronics circuits are located in this housing: the camera trigger board, the video switcher and the strobe fire synchroniser.

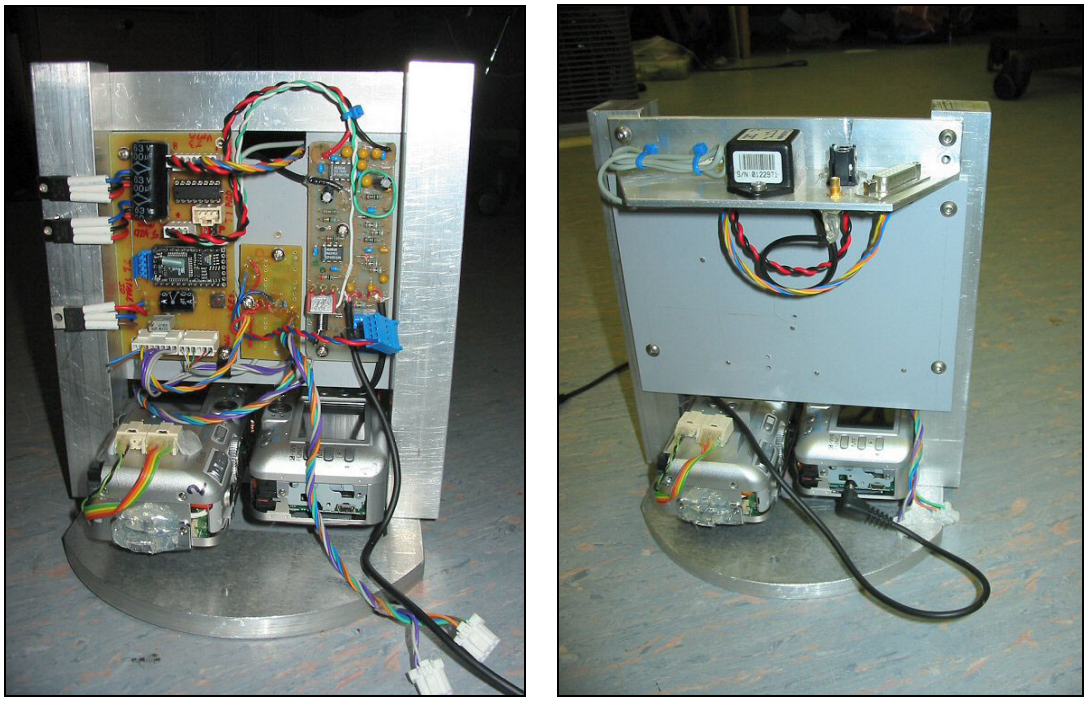

Figure 2(a) and (b): Internals of the Digital Still Stereoscopic Camera (containing two 5 mega-pixel digital still cameras, WEM board, camera trigger board, video switch board, and triaxial accelerometer (inclinometer). (The strobe trigger board was not fitted at the time of this photograph)

The dry-end of the ESP system a laptop computer used to synchronise various systems and to collect data. A custom written computer program called "ESPañolito" performs timing, control, monitoring and data logging functions. It communicates with the GPS, TAPS and WEM via serial port and triggers the EQ60 via a trigger cable.

The user interface of "ESPañolito" is shown in Figure 3. The black area at the top of the screen is where TAPS echosounder data are shown in real-time. "ESPañolito" is written in Labview and also includes some Matlab scripts for data interpretation. The configuration screen of "ESPañolito" is shown in Figure 4. Various settings of hardware interface parameters are shown in this screenshot along with the sampling rate of the cameras and echsounders.

Other pieces of equipment which comprise the dry-end of the ESP system include various power supplies, the top-end PC of the EQ60, the top-end interface box of TAPS, and the RS232/422 converter for the WEM interface, as shown in Appendix 1. A video camcorder is used whilst out in the field for monitoring the video signal from the cameras and recording a video log tape of the deployments. The entire system is powered in the field by a portable 240V generator.

In the field, the ESP wet-end is deployed over the side of the boat on a davit, as pictured in Figure 5. The ESP wet-end is then lowered to an appropriate depth (height above the seafloor) and data logging is commenced. Data were usually collected at a nominal height above the sea floor of 1.5m. However, data were also collected at other distances, either due to vessel movement over variable sea depth or the intentional collection of data at other depths.

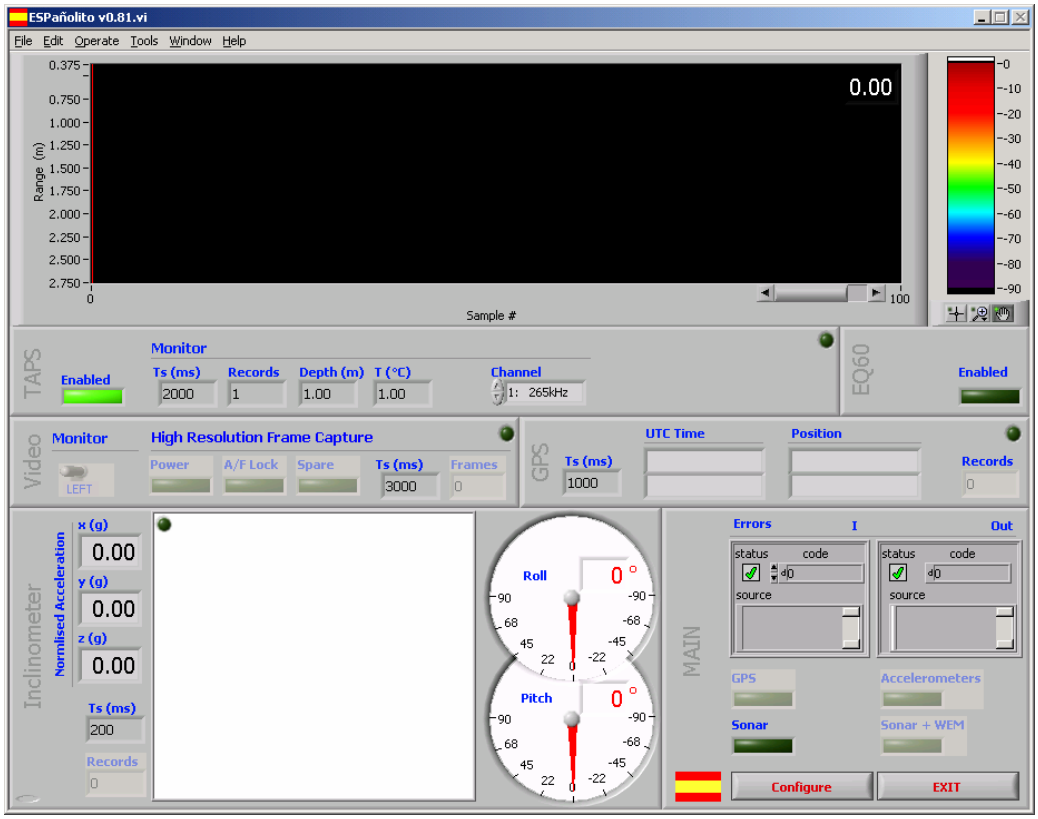

Figure 3: The primary user interface screen of the ESP system software "ESPañolito".

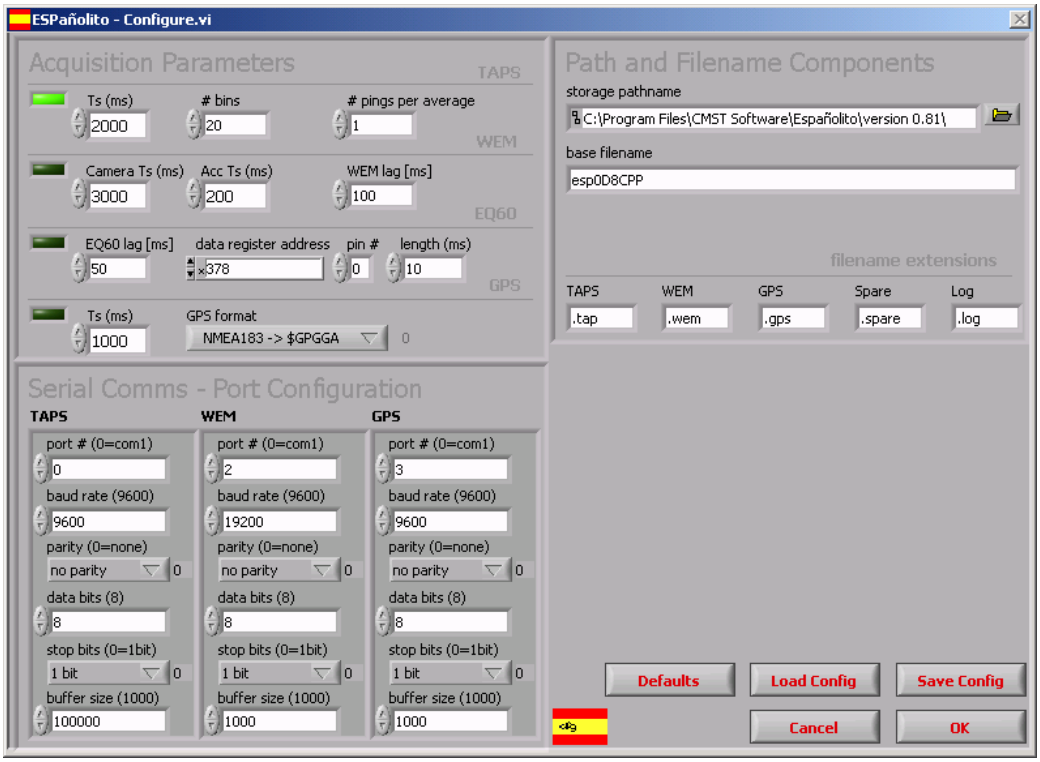

Figure 4: The configuration screen of the ESP system software "ESPañolito".

Figure 5: Davit fitted to boat as used for ESP wet-end deployment
(GPS antenna visible on top of davit)

Experimental Deployments

Three separate field deployments have been conducted with the ESP system:

1. 10th August 2004,
2. 1st June 2005, and
3. 26th October 2005.

The purpose of each of the field deployments is described below:

1. First field deployment: test system operationally and obtain data from various seabed habitat types including particularly sea-grass and sand.
2. Second field deployment: obtain a larger dataset from a range of different seabed habitat types, primarily sea-grass and sand but also algae, reef and mud.
3. Third field deployment: obtain data from a single site which is primarily sea-grass for the full period of the deployment so as to see whether any transpiration effects can be detected. The data collected should also be useful for habitat classification and canopy height/biomass estimation purposes.

An example field itinerary from one of the deployments is given in Appendix 2.

All three experimental deployments were conducted using the vessel “Jabiru” (Figure 6). The setup of some of the dry-end equipment of the ESP system on the back deck of “Jabiru” is shown in Figure 7.

Figure 6: The vessel “Jabiru”.

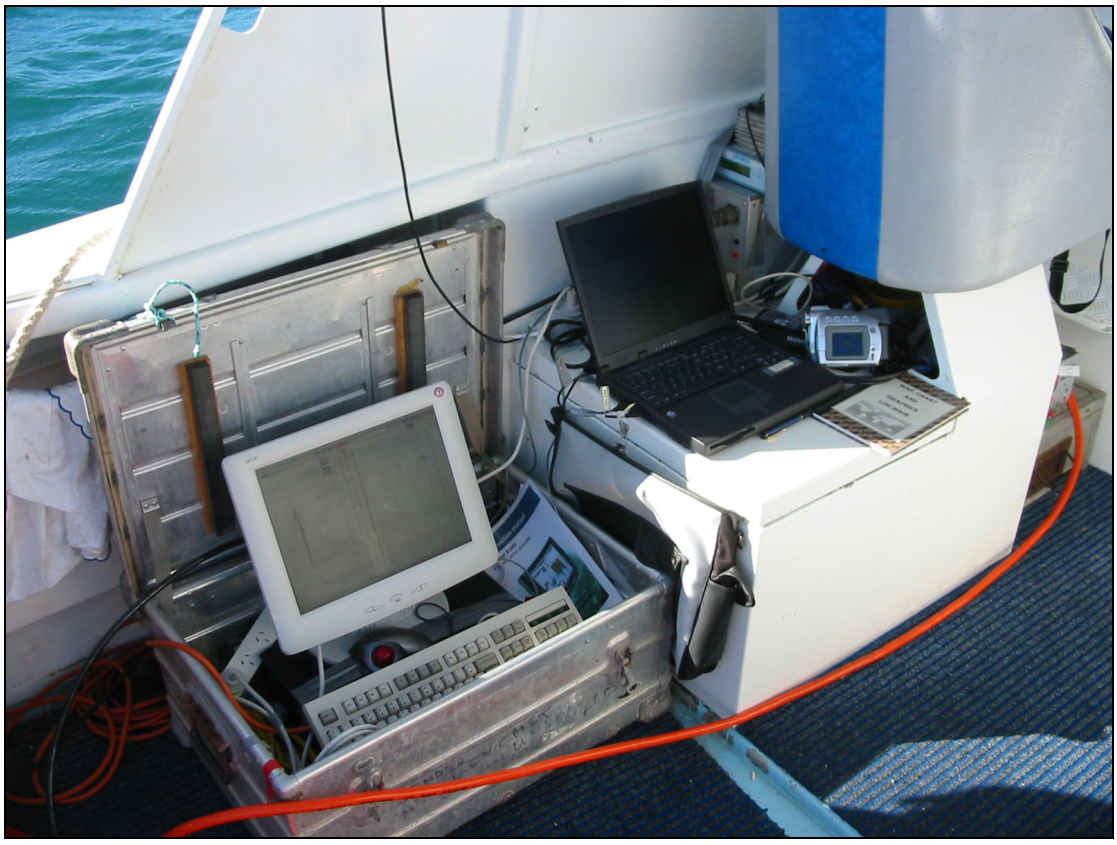

Figure 7: The setup of some of the ESP equipment on the back deck of “Jabiru”.
(EQ60 computer (left), laptop computer running “ESPañolito”, video camera, Omnistar GPS, and various power supplies).

All field deployments were conducted in Cockburn Sound and Owen Anchorage. The GPS locations of all the field survey sites are shown in Table 1. The table also includes a brief description of the seabed at each site. The locations of all the survey sites are also illustrated in Figure 8 and Figure 9.

Table 1: GPS locations of field survey locations for all field deployments

Field Deployment	Site Number	Time	Latitude	Longitude	Seabed Description
First 10th August 2004	Site1	11:30	32° 08.252' S	115° 44.406' E	Seagrass & Sand
	Site 2	12:45	32° 08.251' S	115° 44.414' E	Seagrass & Sand
	Site 3	14:15	32° 09.263' S	115° 45.079' E	Reef and Algae
Second 1st June 2005	Site 1	11:35	32° 07.226' S	115° 45.032' E	Patches of seagrass and patches of rubble
	Site 2	12:00	32° 07.132' S	115° 45.220' E	Patches of seagrass and patches of rubble
	Site 3	12:50	32° 06.323' S	115° 44.215' E	uniform seagrass coverage
	Site 4	14:30	32° 07.649' S	115° 39.830' E	Large algae on rocky seabed
	Site 5	16:00	32° 09.064' S	115° 45.830' E	Muddy seabed
Third 26th October 2005	Site 1	08:30	32° 06.323' S	115° 44.215' E	Seagrass & Sand

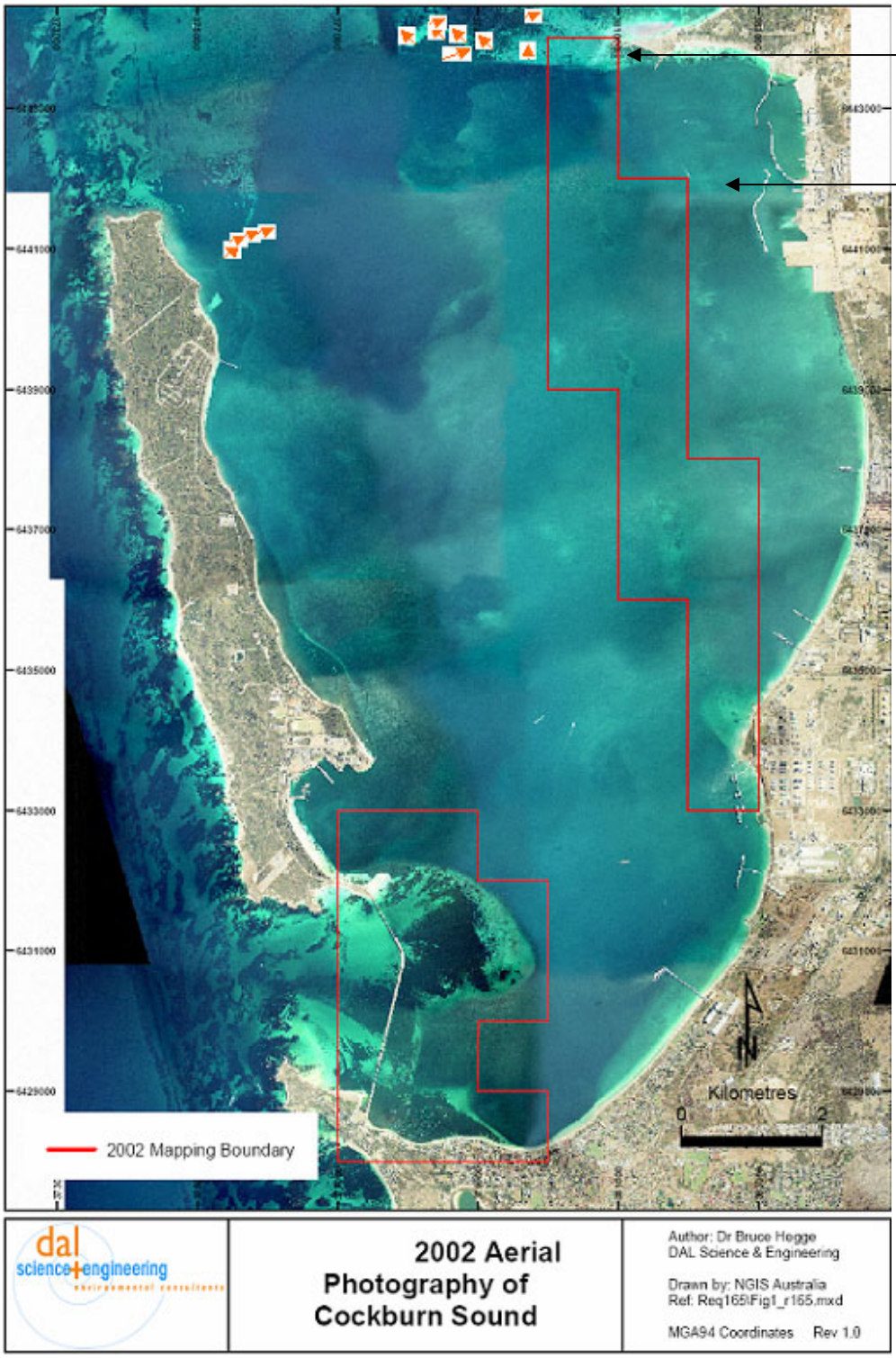

Figure 8: Approximate field survey locations for the first field deployment

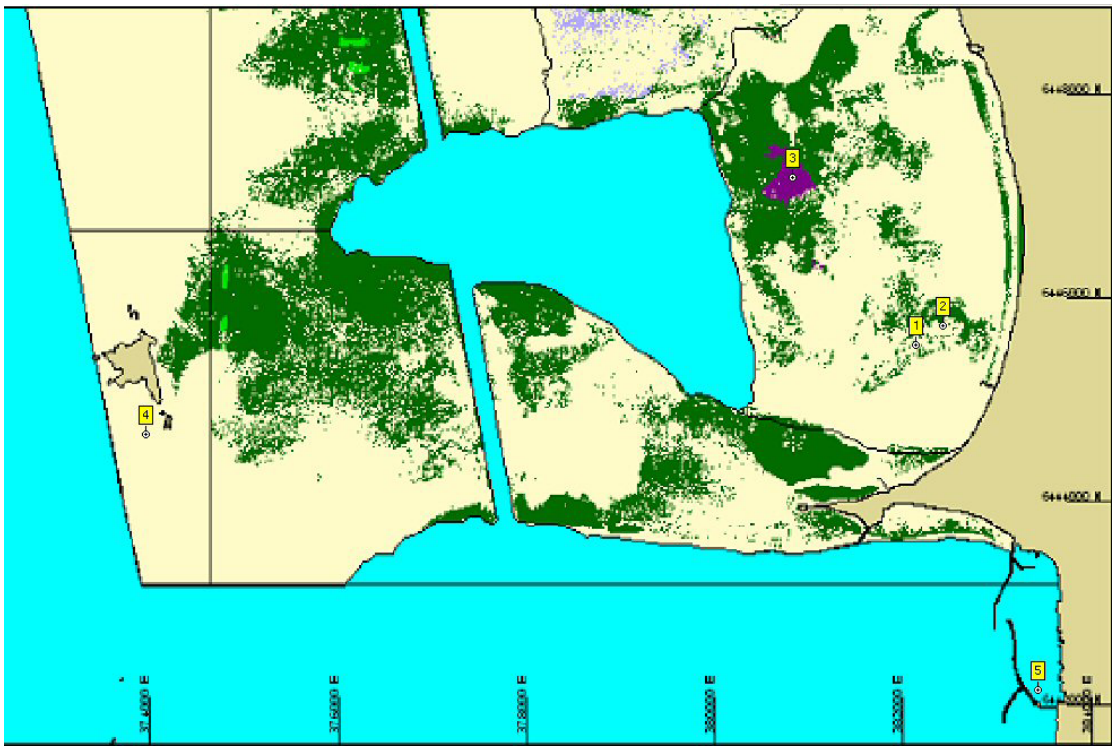

Figure 9: Approximate field survey locations for the second field deployment [1-5] and third field deployment [3] as marked on a seagrass coverage map

Results

The data collected by the ESP system consist of stereoscopic digital still camera images, echosounder backscatter data returns from the EQ60 (two frequencies), echosounder data from TAPS (six frequencies), data from the differential GPS, and accelerometer (inclinometer) data from the WEM.

Examples of stereoscopic images and acoustic data obtained from four different sea floor types as sampled during the first field deployment are shown below in Figures 10-13.

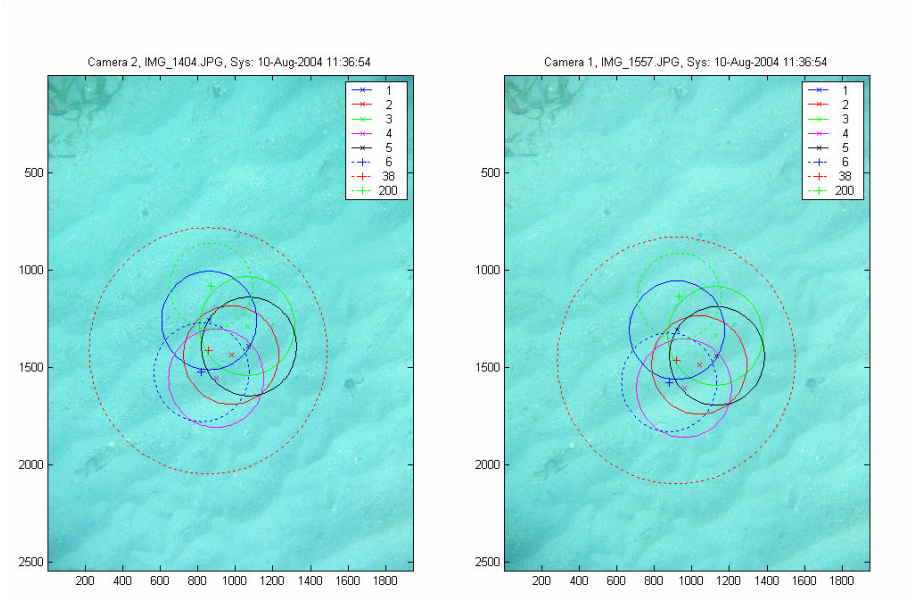

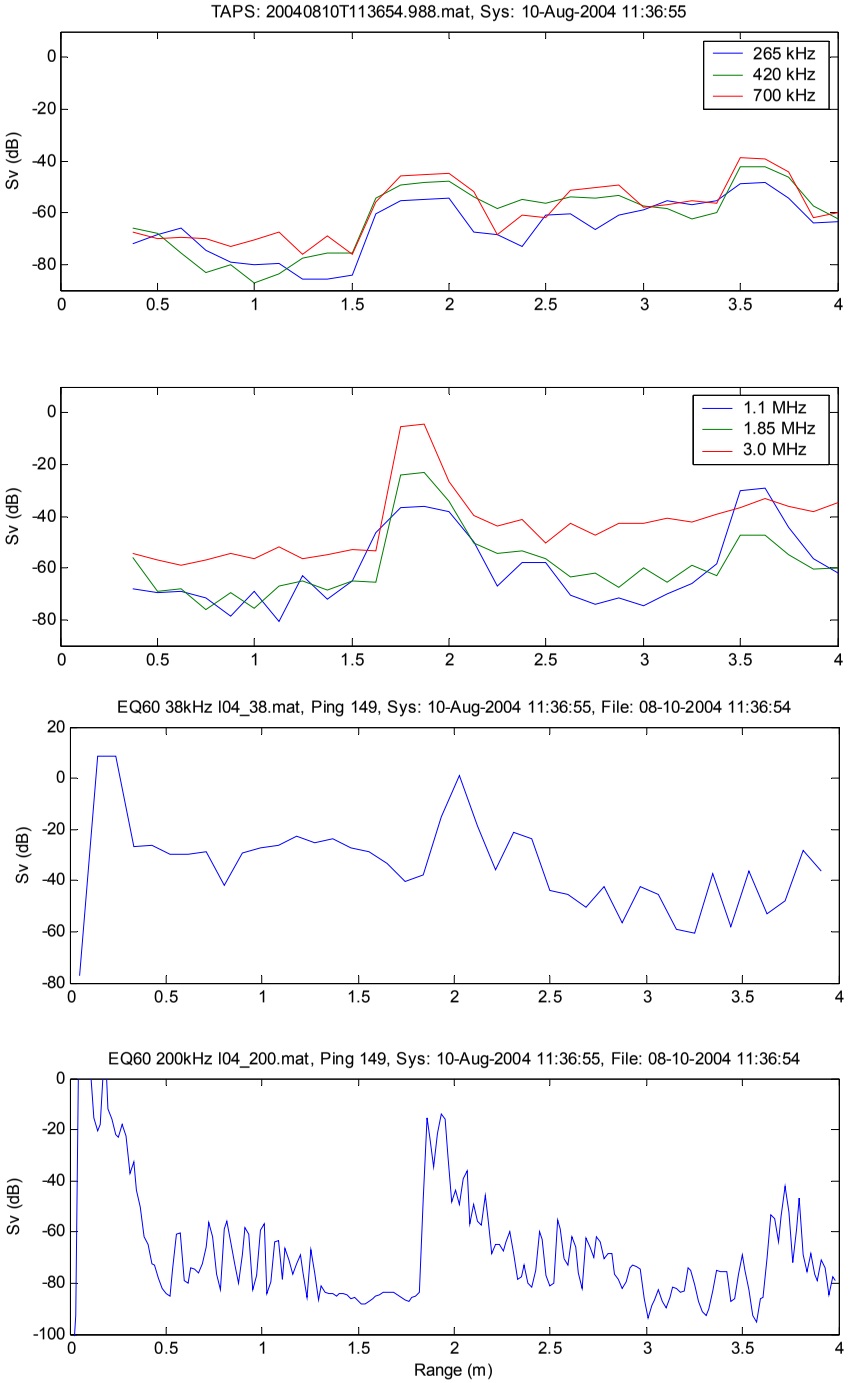

Figure 10: Example stereoscopic image and acoustic backscatter signals for bare sand sea floor

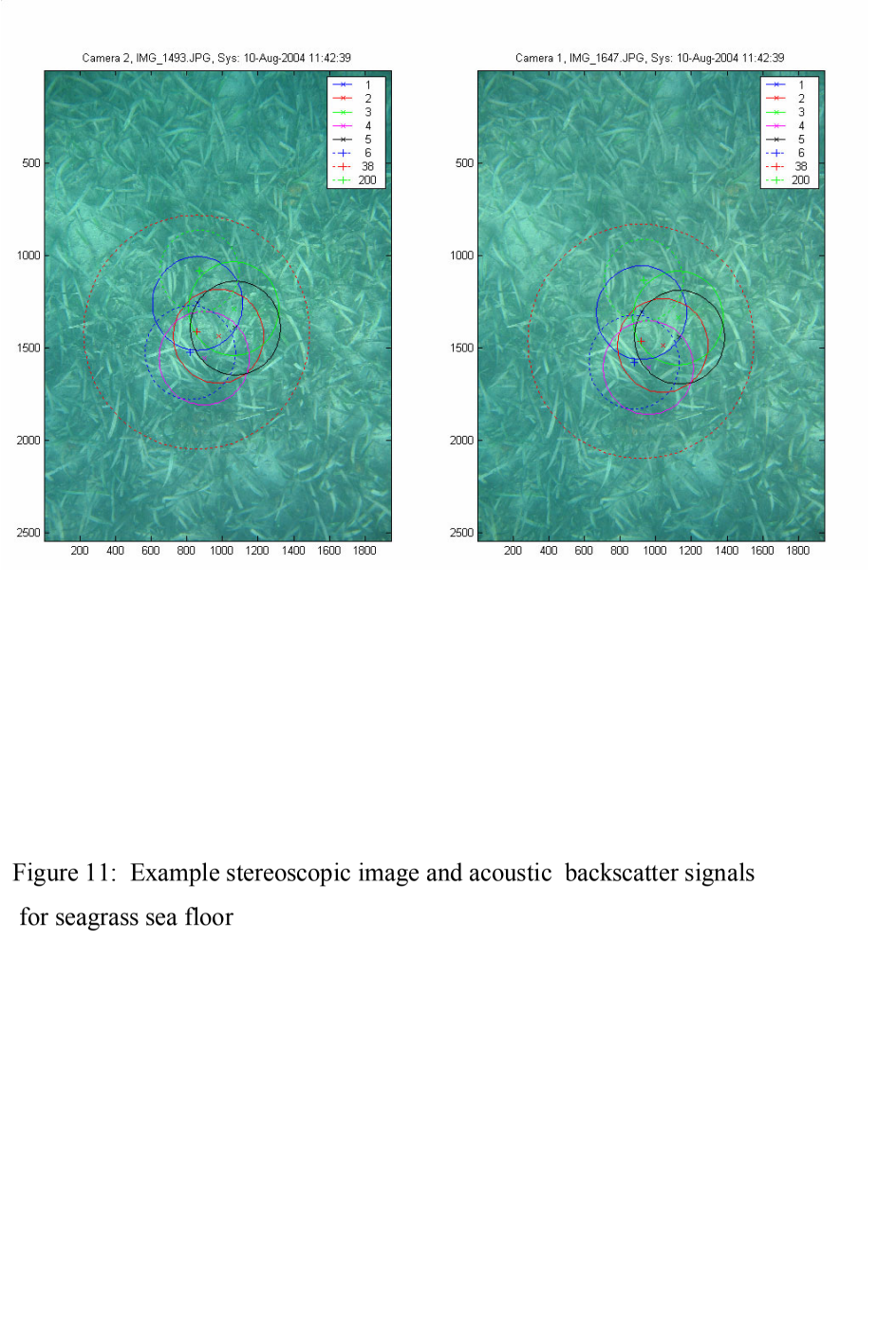

Figure 11: Example stereoscopic image and acoustic backscatter signals for seagrass sea floor

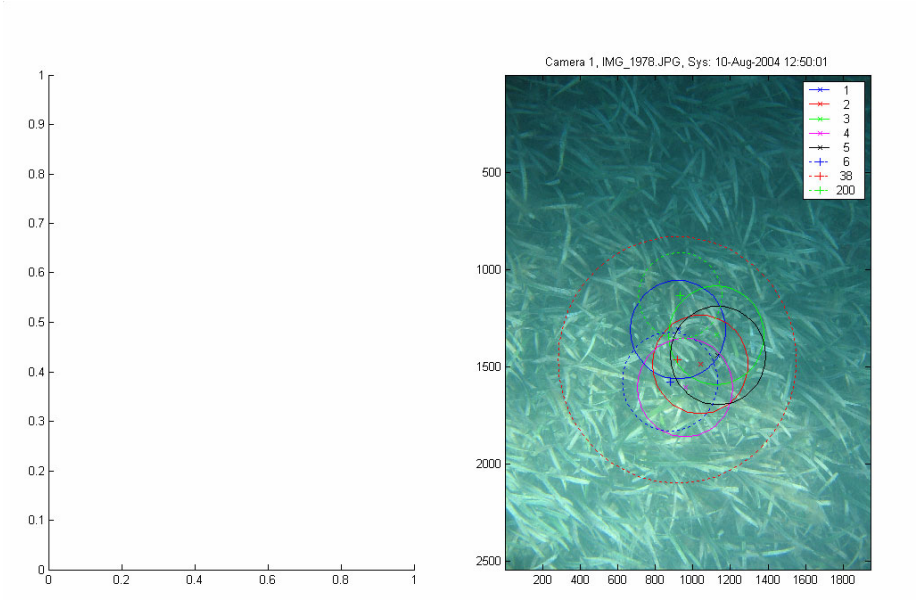

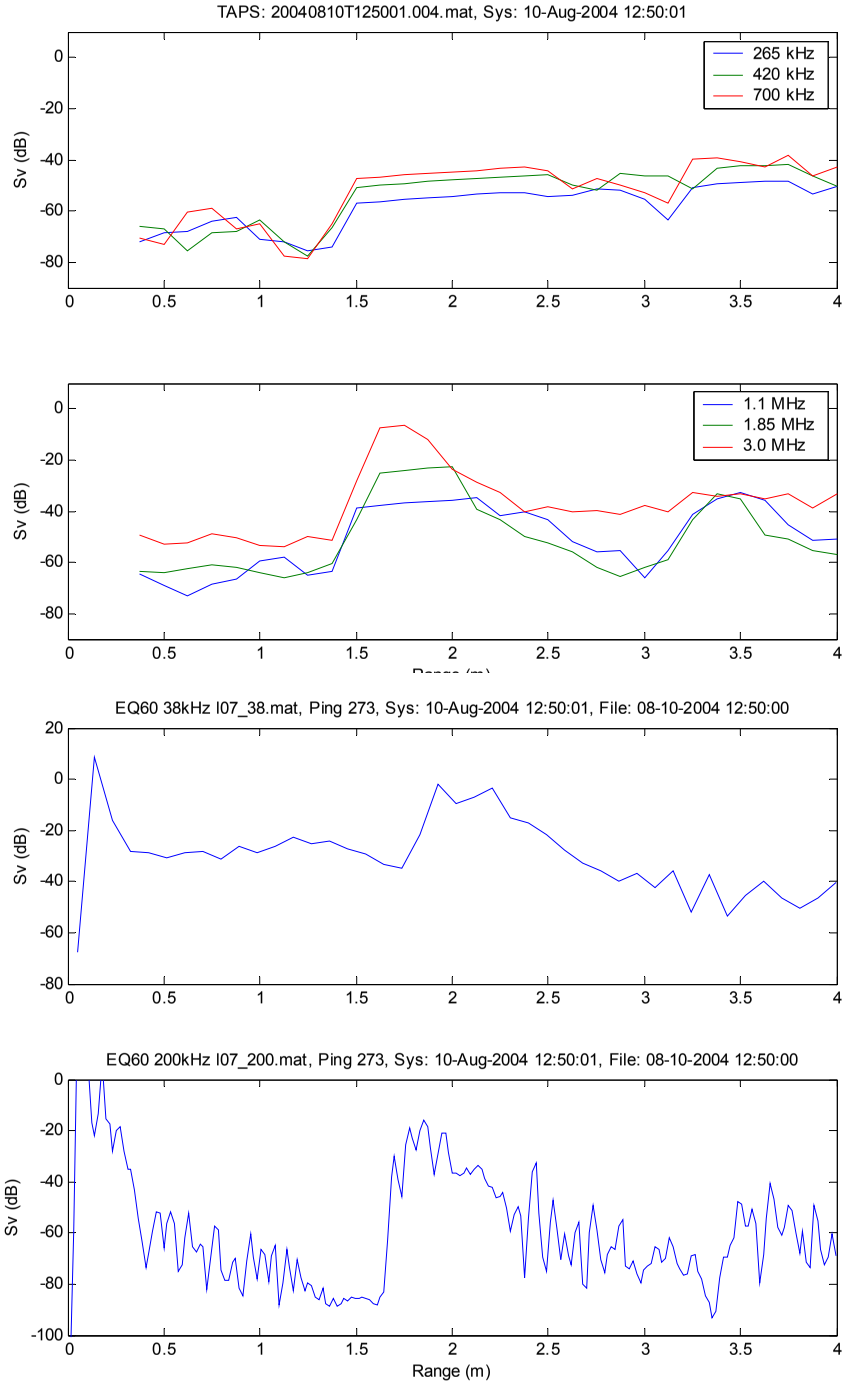

Figure 12: Example stereoscopic image and acoustic backscatter signals for seagrass sea floor

(Note that one pair of the stereoscopic image was not acquired in this case)

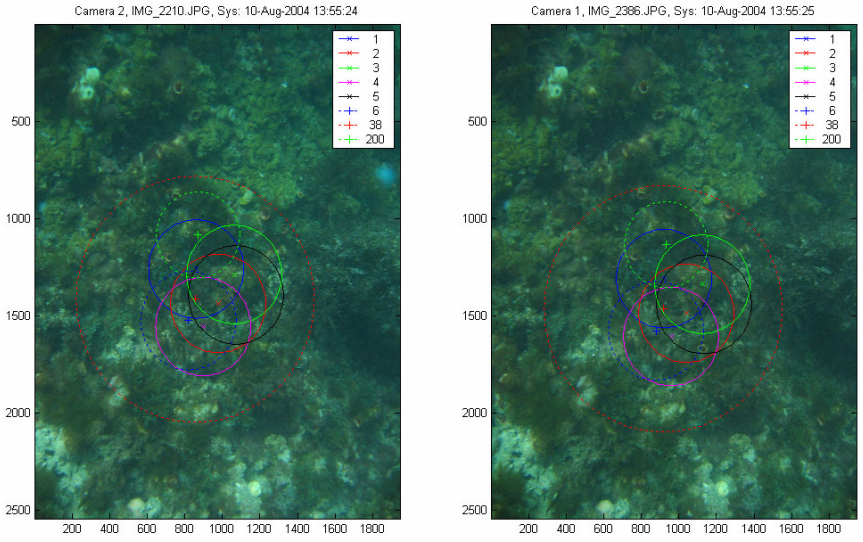

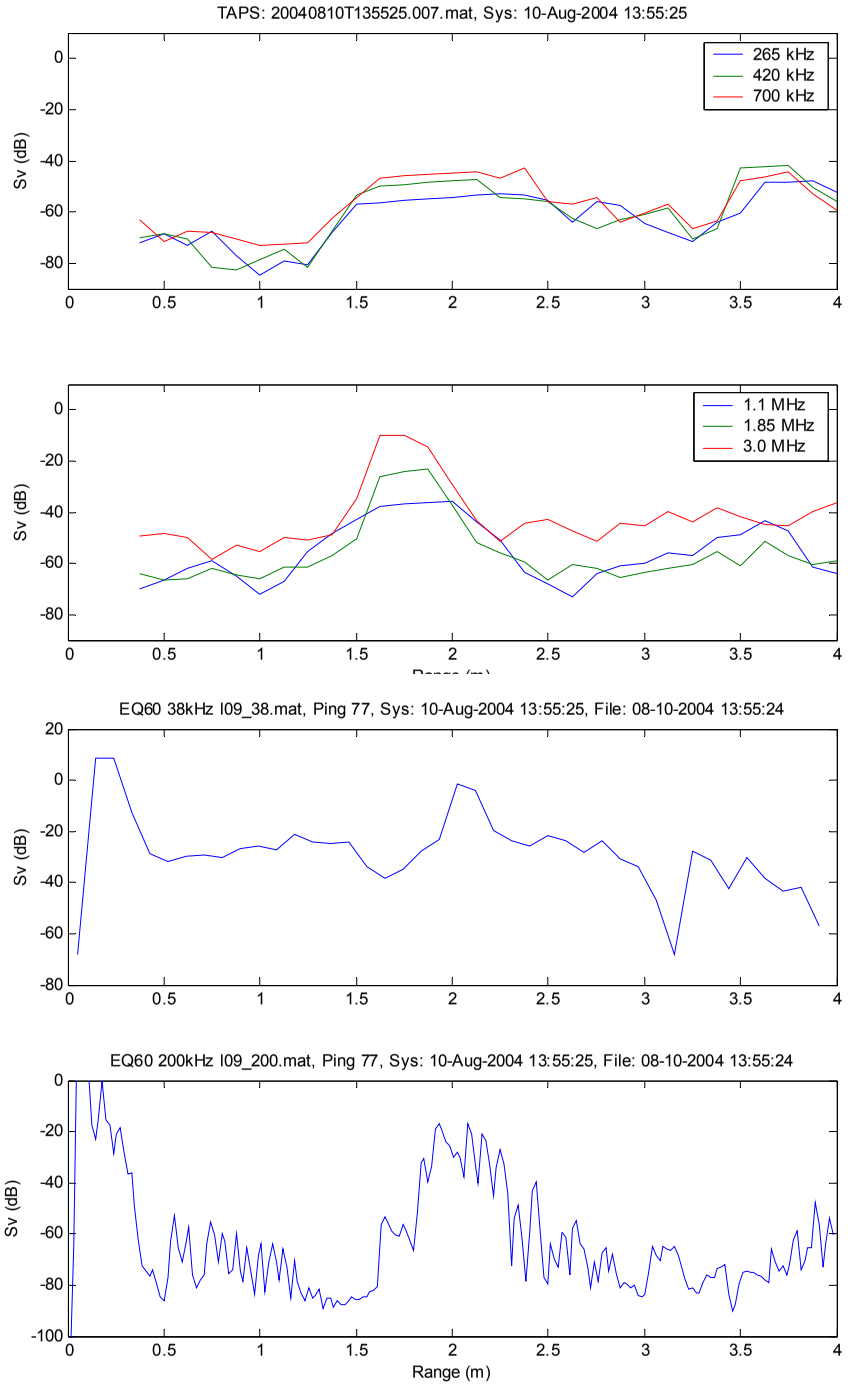

Figure 13: Example stereoscopic image and acoustic backscatter signals for reef sea floor

Data Processing

Synchronisation

Following each field deployment, the raw data were collected onto a PC and backed up. Then the raw binary data from TAP and WEM were converted into a Matlab data format for further processing using the custom program "ESPañolito OPQC".

SonarData ECHO*view* software was used to review and export the EQ60 backscatter data to the Matlab data format. The volume backscattering coefficients exported from ECHO*view* were converted into the surface backscattering coefficients for further analysis.

All of the data were then synchronised in time using a specially written Matlab script to examine the availability of data collected during the trial. An example data availability plot for the first field deployment is shown in Figure 14. The plot shows when data are available from each of the different sensors. Some sensors were turned on and off during the trial so there are cases where not all sensors are available at a particular time. Time on the horizontal axis is indicated in decimal days.

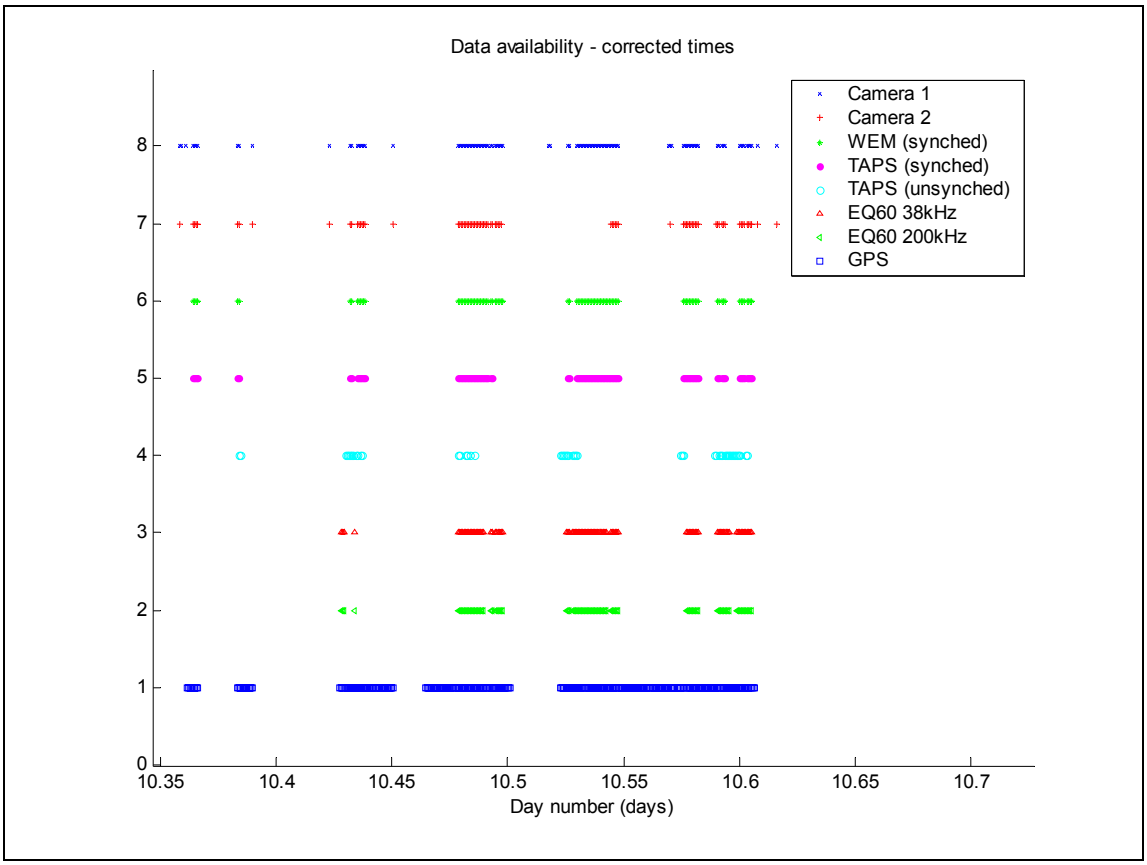

Figure 14: Data availability plot for the first ESP field deployment

The data availability plots can be zoomed on screen to show the correlation of individual data records (pings, images, etc). The Matlab program also provides the

facility to display individual or correlated data records on screen in a manner similar to Figure 10.

Image Classification

In order to provide groundtruthing of the acoustic backscatter data, the underwater stereoscopic images captured during the ESP survey were visually classified by Mr Yao-Ting Tseng. The classification schemes used for the datasets from the three field deployments are listed in Appendix 3. The image classification data were later used in the acoustic data classification training and testing phase described later.

Stereoscopic Alignment

The relative alignment of the stereoscopic camera pair was measured by the use of an alignment target (from UWA) and VMS photogrammetry software (from Mark Shortis). The target consists of 52 accurately located dots on two planes. The target is shown in Figure 15. The target is photographed (in stereo) a total of 20 times in 20 different orientations relative to the cameras. The images are then imported into VMS where the dots in all of the images are located and then the algorithms within VMS determine the relative orientation of the cameras.

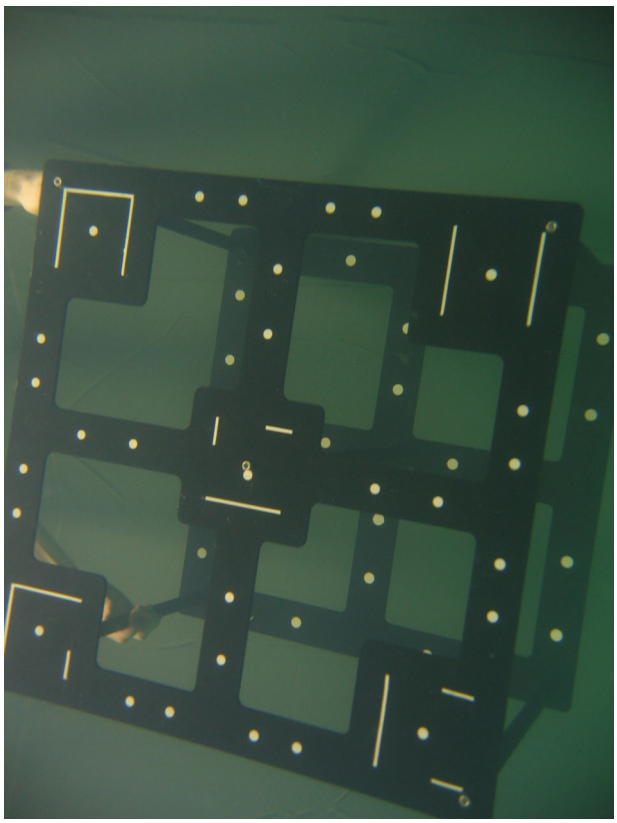

Figure 15: Stereoscopic alignment target

An example stereoscopic camera orientation data output from VMS is shown below:

	Camera 1			Camera 2		
Base	-36.3974	0.000	0.000	36.3974	0.000	0.000
Std Dev	0.0769			0.0769		
Rotations (o,p,k)	0.1832	0.6680	-88.4794	-0.1832	2.1224	91.4984
Std Dev (o,p,k)	0.0021	0.1543	0.1333	0.0021	0.1562	0.1312

These data can be used for measuring height of marine vegetation canopy relative to the substrate in the images. However, limited success has been achieved with this process in the project to date, because the substrate, sand in most cases, is completely hidden under seagrass.

Acoustic Data Interpretation

This section describes the procedure for processing the data from the acoustic systems.

The pulse front of the acoustic backscatter signals was located by finding the first signal sample of which the intensity level exceeded a predefined threshold. It was assumed that backscattering from a seagrass canopy should be stronger at higher frequencies and hence the backscatter signal at 200 kHz should arrive earlier than that at 38 kHz. Once the pulse front was located, the acoustic backscatter characteristics were determined from that backscatter pulse form. In this stage of data analysis, we estimated the following parameters:

Centre of energy i_c

The centre of energy of a pulse is a conventional characteristic to define the centre of pulses of a complicated, stochastically varying form. Its definition is similar to that given in classical mechanics. In the discrete form, the sample index of the centre of energy is defined as

$$i_c(j) = \mathrm{int}\left\{ \sum_i i \cdot f_i(j) \Big/ \sum_i f_i(j) \right\},$$

where f_i are the backscatter pulse samples and the index j denotes the ping number.

Effective pulse width W(*j*)

The effective pulse width is defined as the square root of the second moment of the pulse shape calculated for the pulse magnitude and multiplied by the sampling interval δt, which can be written as follows

$$W(j) = \delta t \sqrt{I(j)}$$

where $I(j) = \sum_i (i - i_c)^2 \cdot f_i(j) \Big/ \sum_i f_i(j)$ is the moment of inertia. The smaller the effective pulse width, the more the backscattered energy will concentrate at the pulse centre.

Surface scattering coefficient s_A

According to Medwin and Clay [9], the surface backscattering coefficient is defined as

$$s_A = P_t R^4 / P_r R_0^2 A ,$$

where A is the insonified area. It is expected that the surface backscattering coefficient for seagrass is smaller at near-nadir angles of incidence than that for sand.

First Field Deployment Data

Figure 16 and Figure 17 demonstrate examples of stereoscopic images of the seafloor taken by the underwater stereoscopic camera over sand and seagrass. Circles show the footprints of the EQ60 and TAPS sonar beams that sampled the seafloor. The stereo-pair images are shown in side-by-side crosseyed format.

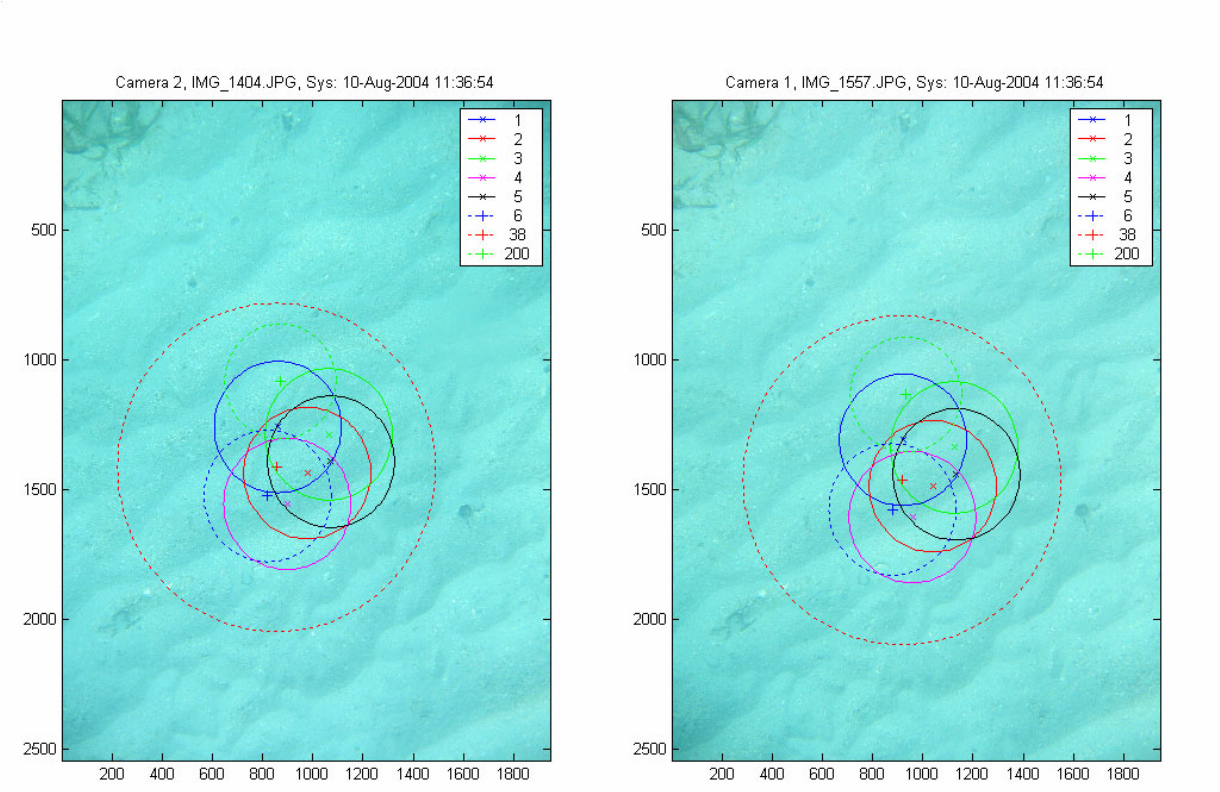

Figure 16: Example of stereoscopic image of bare sand sea floor and footprints of the sonar beams (1-6 - footprints of the TAPS beams at different frequencies; 38 and 200 – footprints of the EQ60 beams at 38 and 200 kHz respectively). Images from first field deployment.

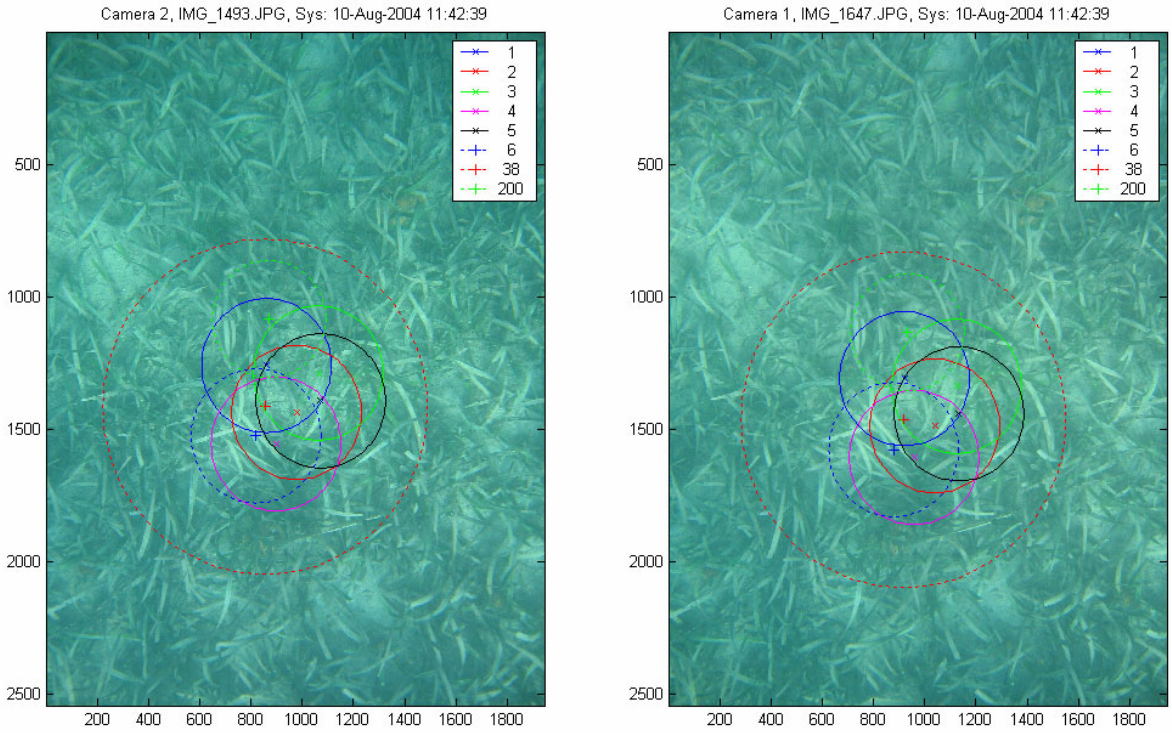

Figure 17: Same as Figure 16, but for seagrass. Images from first field deployment.

The typical pulse form of backscatter signals at 38 and 200 kHz are shown in the top and bottom panels of Figure 18 respectively. The distance from the sonar head to the bottom was approximately 2 m. The high level of backscatter response in the initial 0.5 s time period of recording is the result of decaying ringing of the transducer due to its limited frequency bandwidth.

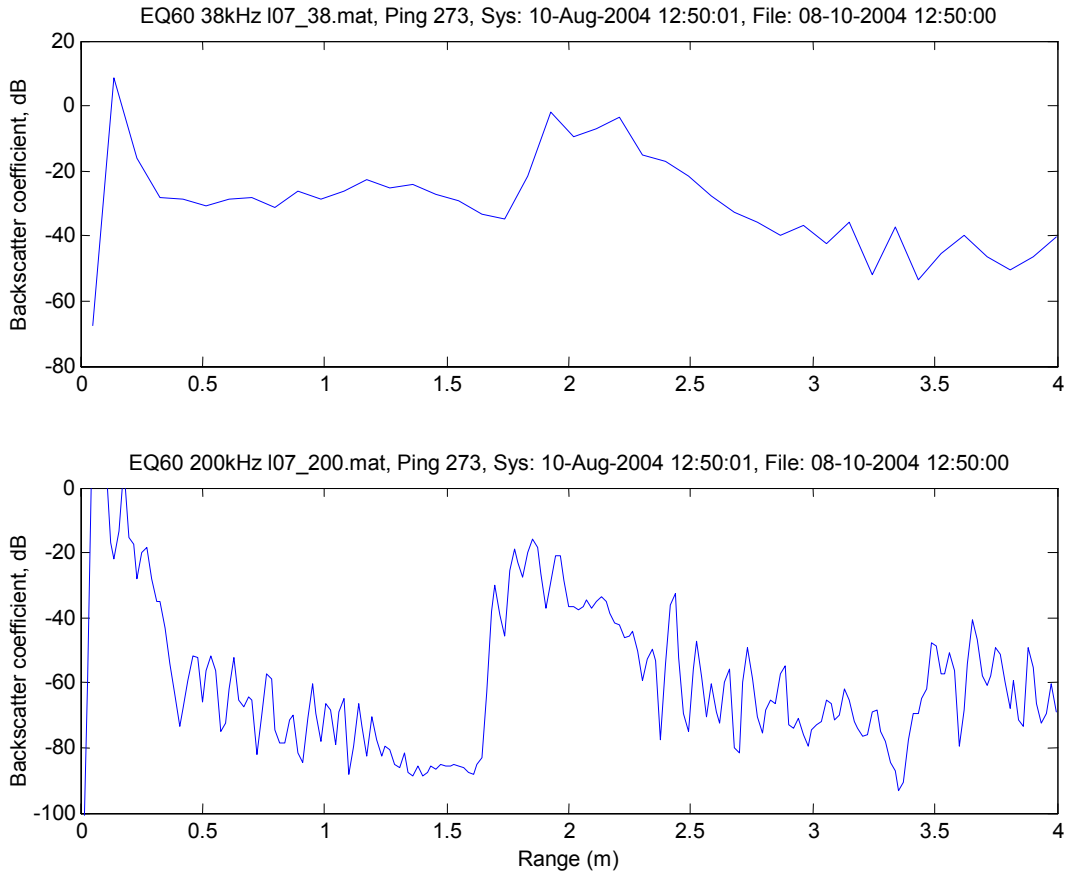

Figure 18: The typical pulse form of backscatter signals at 38 kHz (top) and 200 kHz (bottom). Data from first field deployment.

The distributions of the effective pulse length of backscatter signals at 38 and 200 kHz are shown in Figure 19 and Figure 20 respectively. As can be seen in Figure 19, clustering of backscatter returns from seagrass and sand is problematic at 38 kHz, because the boundary between two classes cannot be definitely established. In contrast to the lower frequency, the effective width of backscatter pulses at 200 kHz can be definitely clustered to discriminate two different seafloor habitats backscattering the sonar pulses.

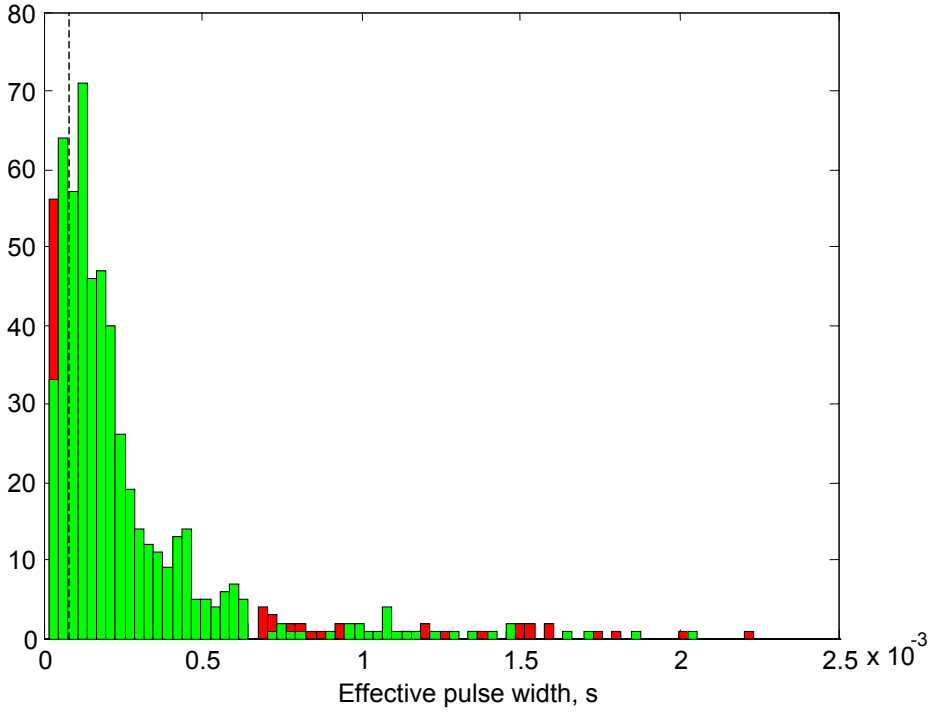

Figure 19: Histogram of the effective pulse width measured at 38 kHz over the seafloor areas covered by sand (red) and sea grass (green) from the first field deployment. Brown columns are an overlap of red and green data.

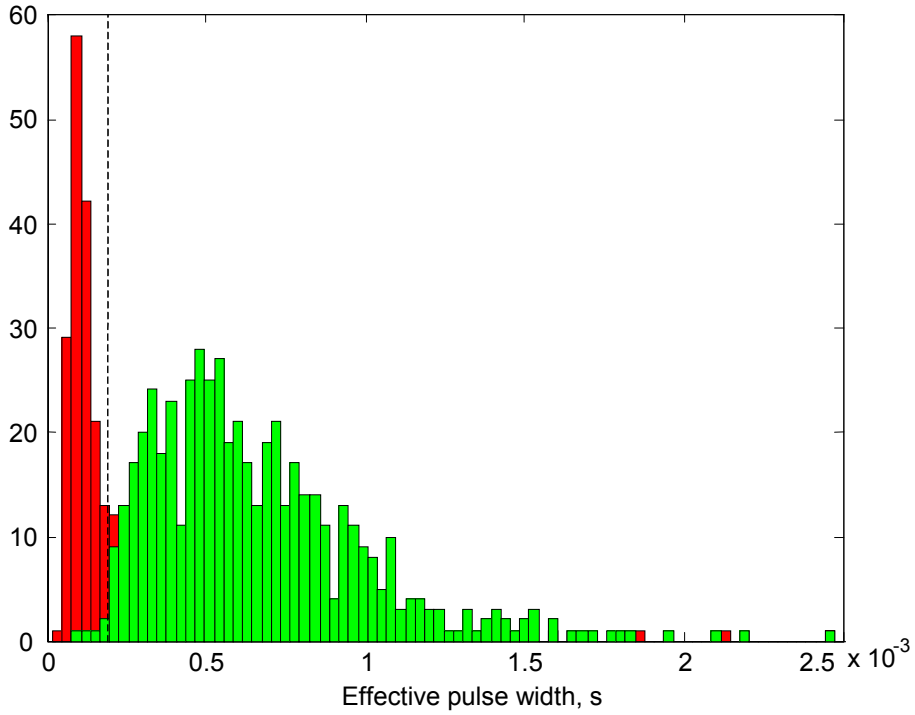

Figure 20: Histogram of the effective pulse width measured at 200 kHz over the seafloor areas covered by sand (red) and seagrass (green) from the first field deployment. Brown columns are an overlap of red and green data.

Figure 21 shows the distribution of seagrass and sand patches along the survey tracks within the first and second area of the first field deployment. The left panel displays the actual distribution of seagrass obtained from the stereoscopic camera data. The middle panel shows the reconstruction of seagrass distribution derived from acoustic observations at 200 kHz through clustering the samples by the effective pulse width. The efficiency of acoustic recognition of seagrass at 200 kHz is quite high: only 7 per cent of samples were false detections of seagrass. Recognition of seagrass using the backscatter returns at 38 kHz is substantially less confident, which is seen in the right panel of Figure 21.

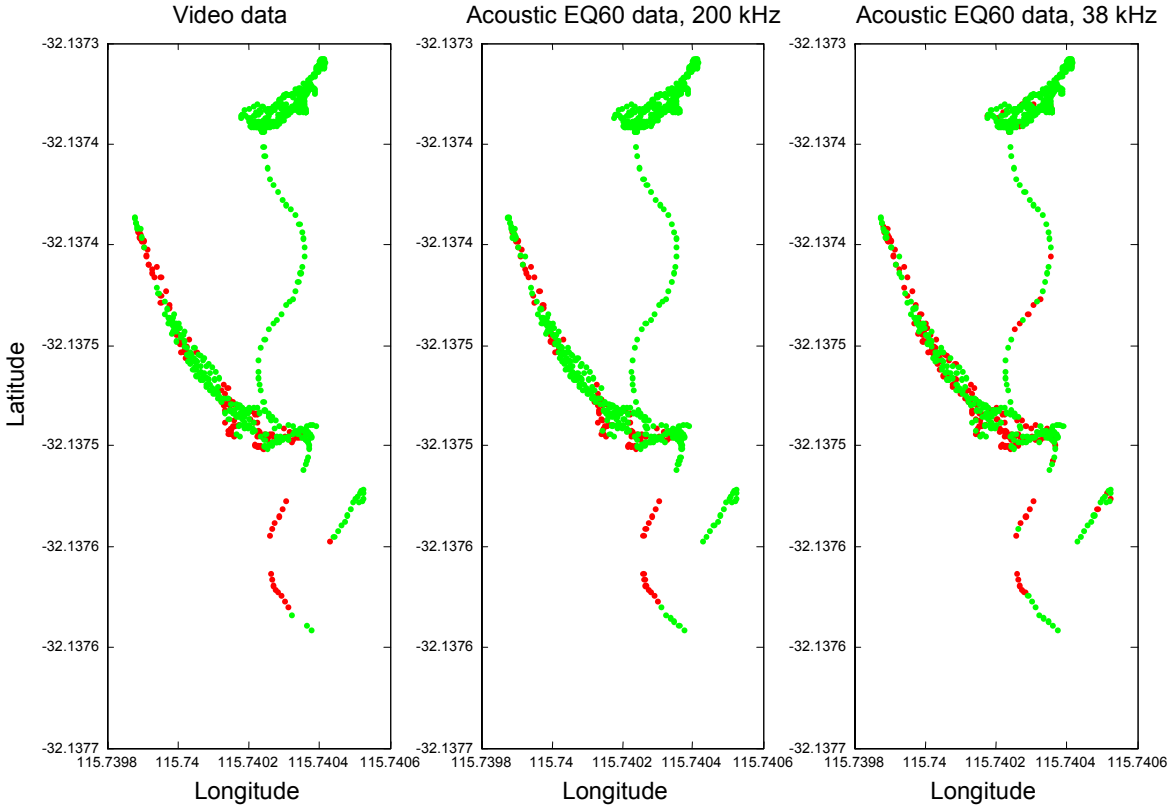

Figure 21: Distribution of seagrass and sand along the survey tracks (from area 1 and 2 of the first field deployment) in Cockburn Sound determined visually from underwater digital still stereoscopic camera images (left panel) and reconstructed from the EQ-60 sonar data at 200 kHz (middle panel) and 38 kHz (right panel) by segmentation of the effective pulse width of backscatter signals. The false detection rate of acoustic soundings for seagrass is about 7 per cent at 200 kHz.

Second Field Deployment Data

Figures 22 to 25 show the classification of the survey areas of the second field deployment by two basic classes (seagrass and sand (non-seagrass)). In Figures 22 to 25, the upper panel displays the actual distribution of seagrass obtained from the stereoscopic camera images. The lower panel shows the reconstruction of seagrass distribution derived from acoustic observations at 200 kHz through clustering the

samples by the effective pulse width. An effective pulse width threshold of 0.000225 seconds has been used for these figures. Figures 23 to 25 show enlargements of the three areas indentified in Figure 22.

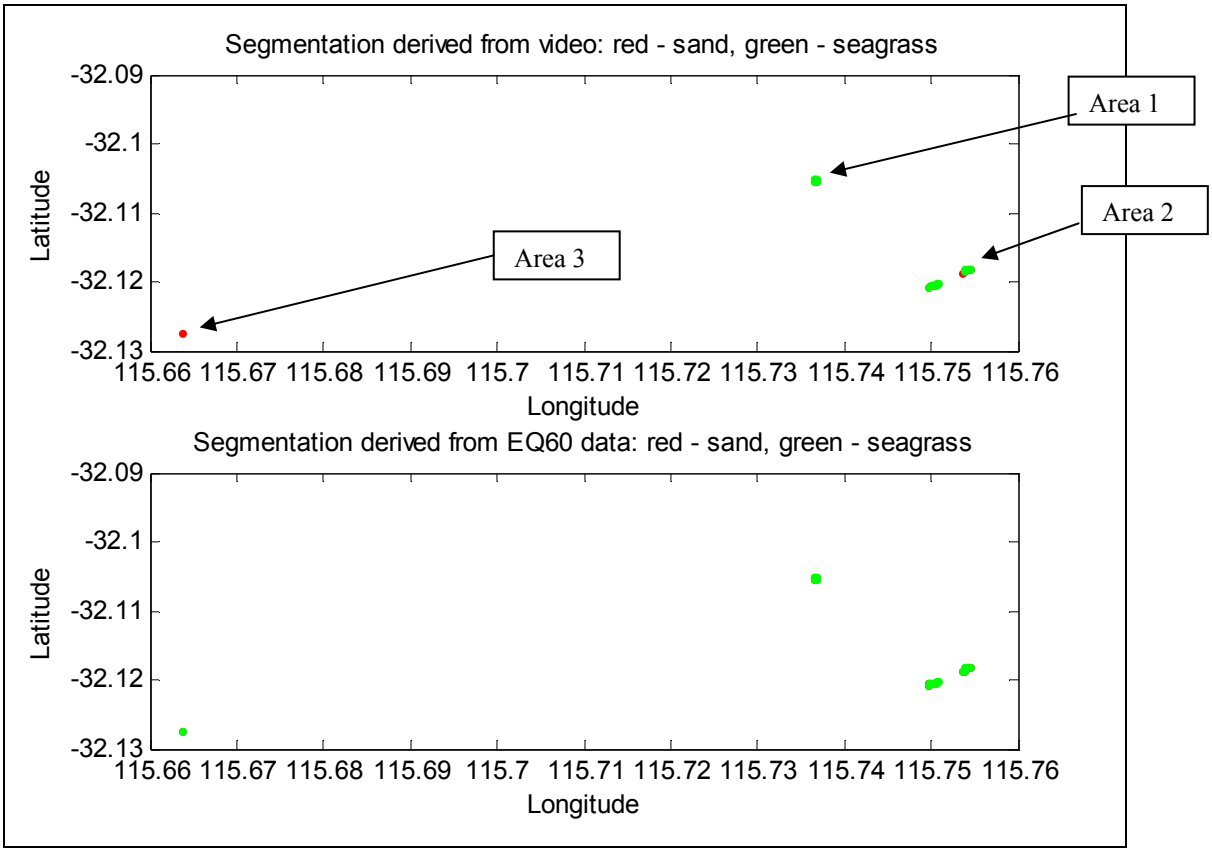

Figure 22: Distribution of seagrass and sand along the survey tracks of the second field deployment in Cockburn Sound determined visually from underwater digital still stereoscopic camera images (upper panel) and reconstructed from the EQ-60 sonar data at 200 kHz (lower panel) by segmentation of the effective pulse width of backscatter signals.

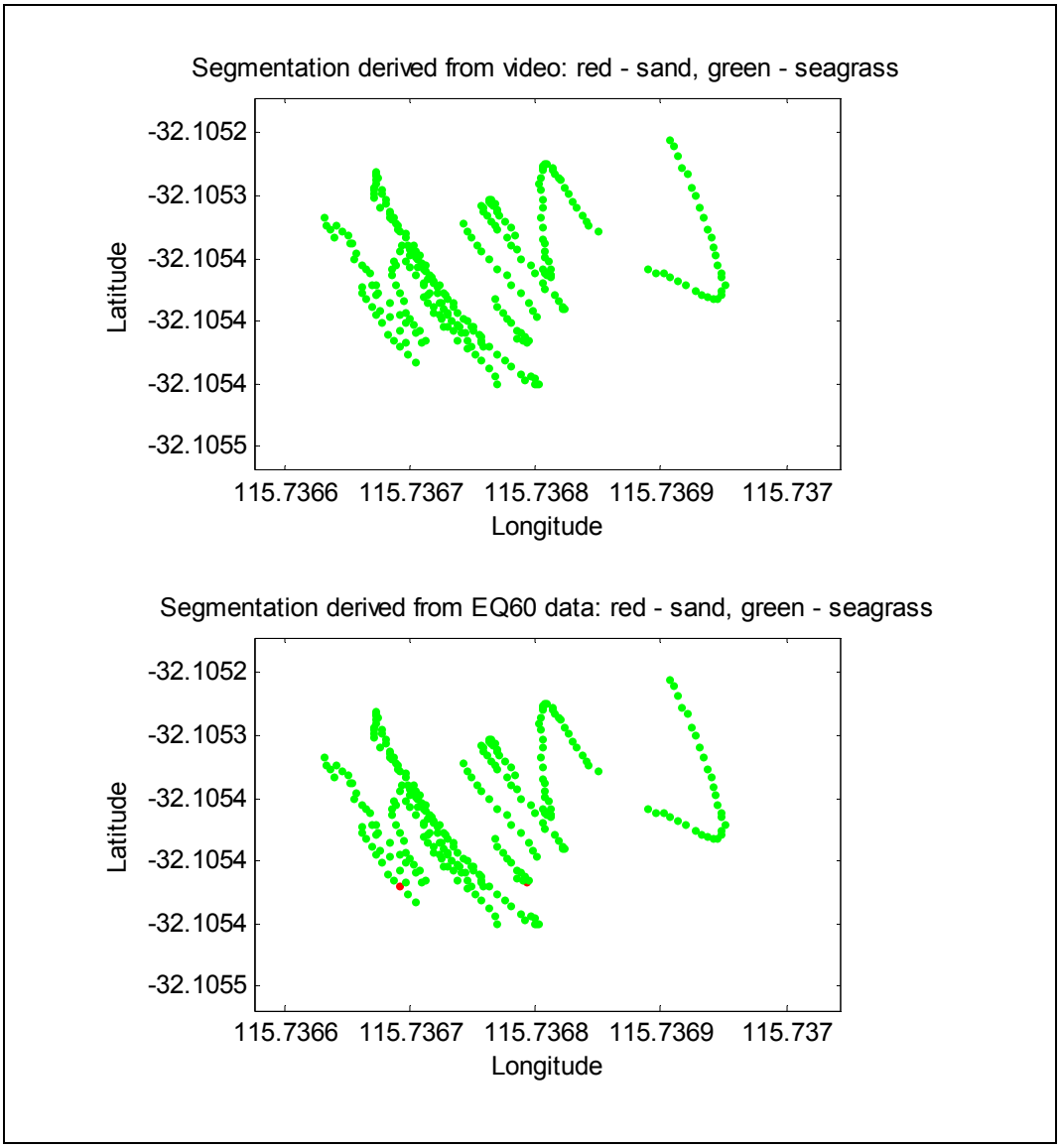

Figure 23: Enlargement of Area 1 from Figure 22. Visual classification in upper panel and acoustic classification in lower panel.

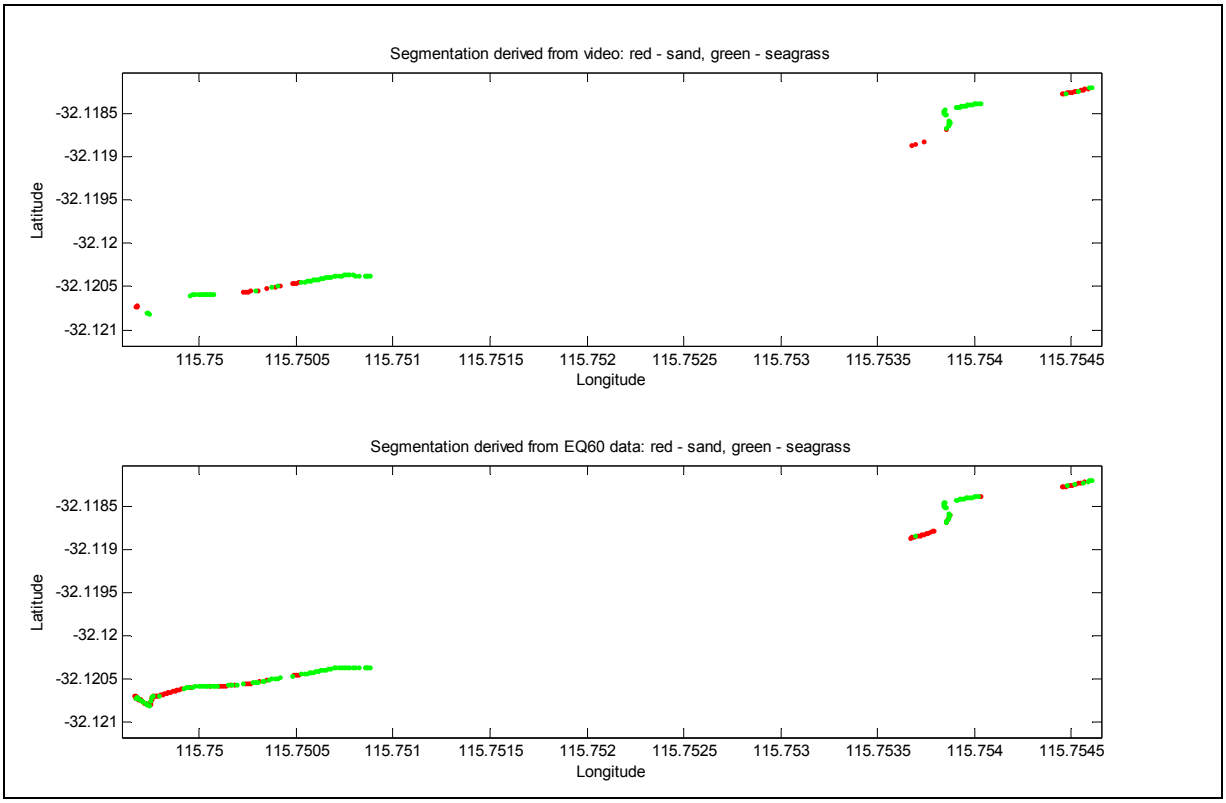

Figure 24: Enlargement of Area 2 from Figure 22. Visual classification in upper panel and acoustic classification in lower panel.

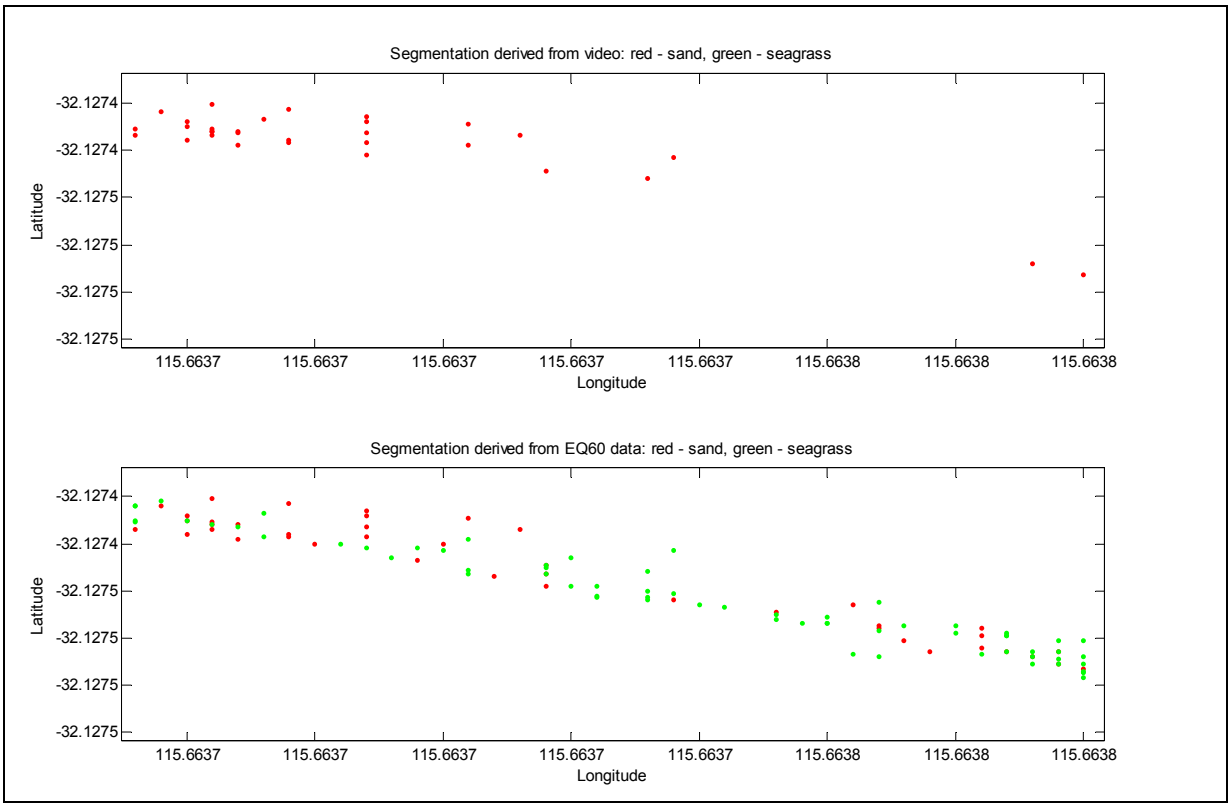

Figure 25: Enlargement of Area 3 from Figure 22. Visual classification in upper panel and acoustic classification in lower panel.

The success rate of acoustic classification (using effective pulse width with a threshold at 0.000225 seconds for 200kHz) is shown below in Tables 2 and 3. The green highlighted cells indicate the number of records where the acoustic classification method has correctly identified the seafloor habitat type (between the two classes seagrass and sand). The efficiency of acoustic recognition of seagrass at 200 kHz is quite high - only 5 per cent of the pure samples were false detections. Pure samples are those which only contain a particular class type – i.e. there is no mixing.

Table 2: Classification results for the data collected in the second field deployment (for pure image classes only).

Pure classes:		Image		
		Sand 29	Seagrass 162	Other 833
Acoustics	Class1(Sand) 362	21/29	1/162	340/833
	Class2(Seagrass) 662	8/29	161/162	493/833

Table 3: Classification results for the data collected in the second field deployment (for all image classes generalised to seagrass and sand).

General classes:		Image		
		Sand 101	Seagrass 380	Other 543
Acoustics	Class1(Sand) 362	61/101	10/380	291/543
	Class2(Seagrass) 662	40/101	370/380	252/543

Third Field Deployment Data

Figures 26 to 28 show the classification results for the survey areas of the second field deployment using two basic classes (seagrass and sand (non-seagrass)). In Figures 26

to 28 the upper panel displays the actual distribution of seagrass obtained from the stereoscopic camera images. The lower panel shows the reconstruction of seagrass distribution derived from acoustic observations at 200 kHz through clustering the samples by the effective pulse width. An effective pulse width threshold at 0.000225 seconds has been used for these figures. Figures 27 and 28 show enlargements of the three areas indentified in Figure 26.

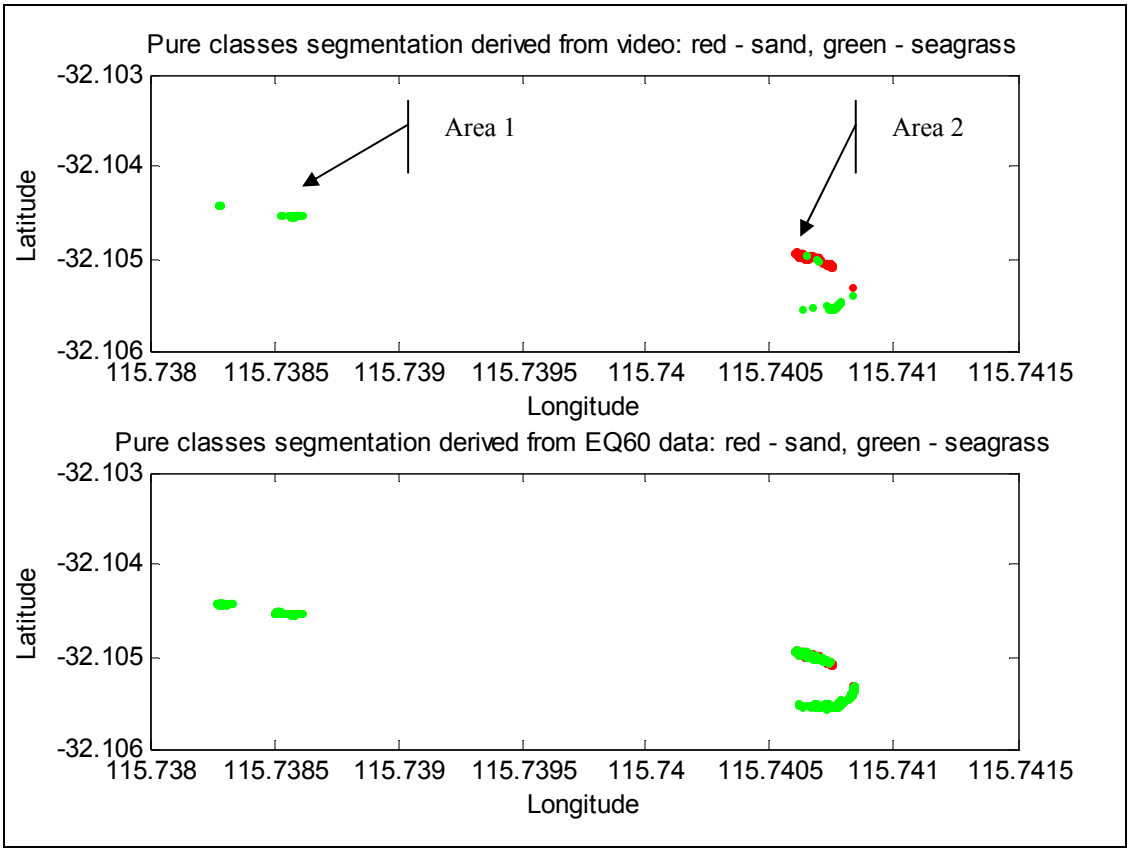

Figure 26: Distribution of seagrass and sand along the survey tracks of the third field deployment in Cockburn Sound determined visually from underwater digital still stereoscopic camera images (upper panel) and reconstructed from the EQ-60 sonar data at 200 kHz (lower panel) by segmentation of the effective pulse width of backscatter signals.

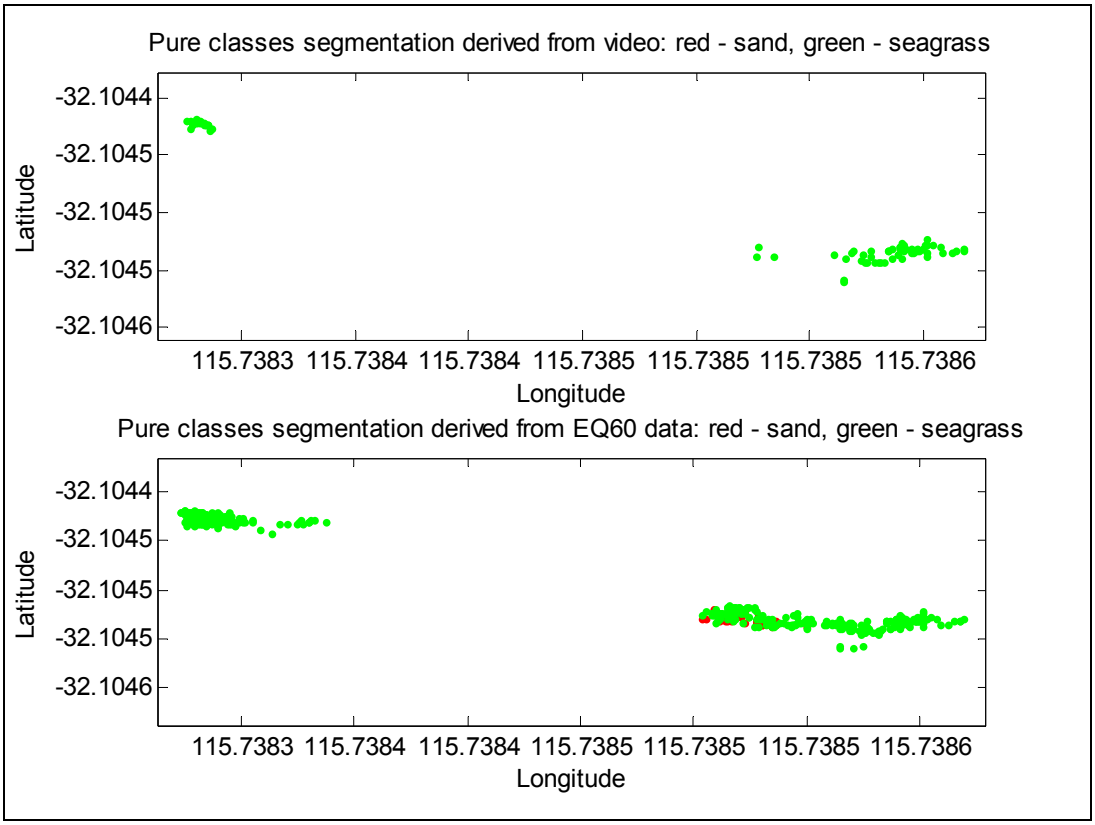

Figure 27: Enlargement of Area 1 from Figure 26. Visual classification upper panel and acoustic classification lower panel.

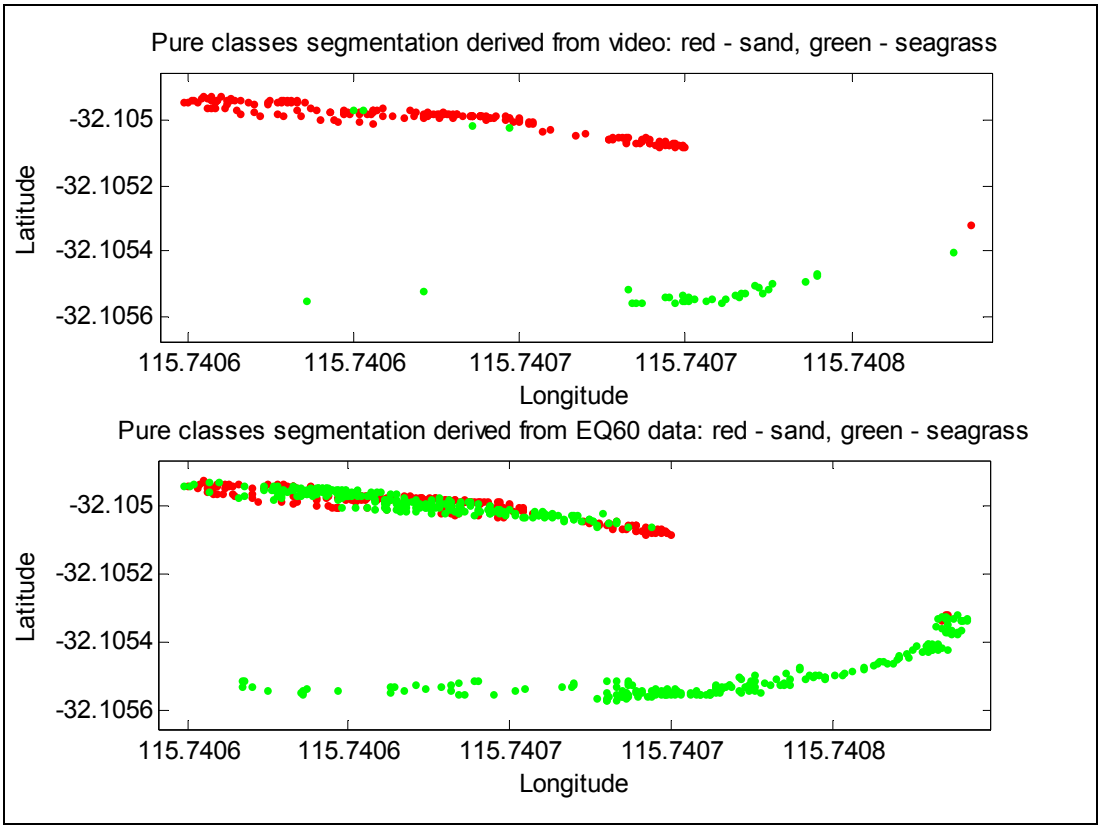

Figure 28: Enlargement of Area 2 from Figure 26. Visual classification upper panel and acoustic classification lower panel.

The success rate of the acoustic classification (using effective pulse width with a threshold at 0.000225 seconds for 200kHz) for the third field deployment data is shown below in Tables 4 and 5. The green highlighted cells indicate the number of records where the acoustic classification method has correctly identified the seafloor habitat type (between seagrass and sand). The efficiency of acoustic recognition of seagrass at 200 kHz is relatively good - only 15 per cent of the pure samples were false detections. It should however be noted that the effective pulse width threshold value used for these tables was not optimised and further improvements are to be expected from further analysis of the data.

Table 4: Classification results for the data collected in the third field deployment (for pure image classes only).

Pure classes:		Image		
		Sand 178	Seagrass 115	Other 891
Acoustics	Class1(Sand) 255	133/178	1/115	121/891
	Class2(Seagrass) 929	45/178	114/115	770/891

Table 5: Classification results for the data collected in the third field deployment (for all image classes generalised to seagrass and sand).

General classes:		Image		
		Sand 241	Seagrass 644	Other 299
Acoustics	Class1(Sand) 255	165/241	86/644	4/299
	Class2(Seagrass) 929	76/241	558/644	295/299

Conclusion

The ESP system described in this report has achieved its goal of simultaneous acoustic and optical sampling of the seafloor habitats (to the extent allowed by the available acoustic hardware). This has resulted in a unique data set in which the acoustic data are fully groundtruthed by high-resolution stereo image pairs. At the time of writing this report, the project had revealed some important results with respect to acoustic discrimination of seagrass from sand in areas of Cockburn Sound. The dataset collected by the field deployment stages of the project has not yet been fully processed to conclude whether more advanced levels of classification are possible – particularly the extension of the algorithms to discriminate other seabed classes and, in particular, the determination of other seagrass properties such as canopy height.

References

Milestone Reports

A.J. Woods, A.J. Duncan, Y-T Tseng, M.A. Perry (2004) "Epibenthic Scattering Project (ESP): Experimental Design Report", Coastal CRC Milestone Report CA2.03.

A.J. Woods, A.J. Duncan, Y-T Tseng, R.D. McCauley, A.N. Gavrilov (2004) "Epibenthic Scattering Project (ESP): Report of First Field Deployment" Coastal CRC Milestone Report CA3.05.

A.N. Gavrilov, A.J. Woods, A.J. Duncan, Y-T Tseng, M.A. Perry, R.D. McCauley (2005) "Epibenthic Scattering Project (ESP): Data Analysis from First ESP Field Deployment and recommendations", Coastal CRC Milestone Report CA4.03.

A.J. Duncan, A.J. Woods, Y-T Tseng, M.A. Perry, R.D. McCauley, A.N. Gavrilov (2005) "Epibenthic Scattering Project (ESP): Report of Second Field Deployment", Coastal CRC Milestone Report CA5.04.

A.J. Woods, A.J. Duncan, Y-T Tseng, A.N. Gavrilov (2005) "Epibenthic Scattering Project (ESP): Report of Third Field Trial", CRC Milestone Report CA5.04 supplement.

Conference Papers

Gavrilov, A.N., Duncan, A.J. , McCauley R.D., Parnum, I. M., Penrose, J.D., Siwabessy, P.J.W., Woods, A.J., Y-T. Tseng (2005). Characterization of the seafloor in Australia's Coastal zone using acoustic techniques. Proceedings of the International Conference "Underwater Acoustic Measurements: Technologies & Results" Heraklion, Crete, Greece, 28th June – 1st July 2005

Y.-T. Tseng, A.N. Gavrilov, A.J. Duncan (2005) Classification of acoustic backscatter from marine macro-benthos. Conference Proceedings, "Boundary

influences in high frequency, shallow water acoustics" conference, University of Bath, UK, 5th-9th September 2005

Y.-T. Tseng, A.N. Gavrilov, A.J. Duncan, M. Harwerth, S. Silva (2005) Implementation of Genetic Programming toward the Improvement of Acoustic Classification Performance for Different Seafloor Habitats. IEEE Oceans 2005

Y.-T. Tseng, (2005) settings of genetic programming toward the Improvement of acoustic classification performance For different seafloor conditions Proceedings of the International Conference "Underwater Acoustic Measurements: Technologies & Results" Heraklion, Crete, Greece, 28th June – 1st July 2005

Acknowledgements

The team working on the ESP project would like to acknowledge the following companies and individuals who have contributed to the project: Coastal CRC, Fugro Survey (Cass Castinanelli, Bill Russell-Cargill - Differential GPS system), Sonardata (Tim Pauly - Echoview software), University of Melbourne (Mark Shortis - VMS software), CSIRO Marine Research (Tony Koslow, Nic Mortimer - loan of TAPS), UWA (Euan Harvey, Dave Gull – Alignment frame and), and the owners of *Jabiru.*

Appendix 1:
ESP System Block Diagram

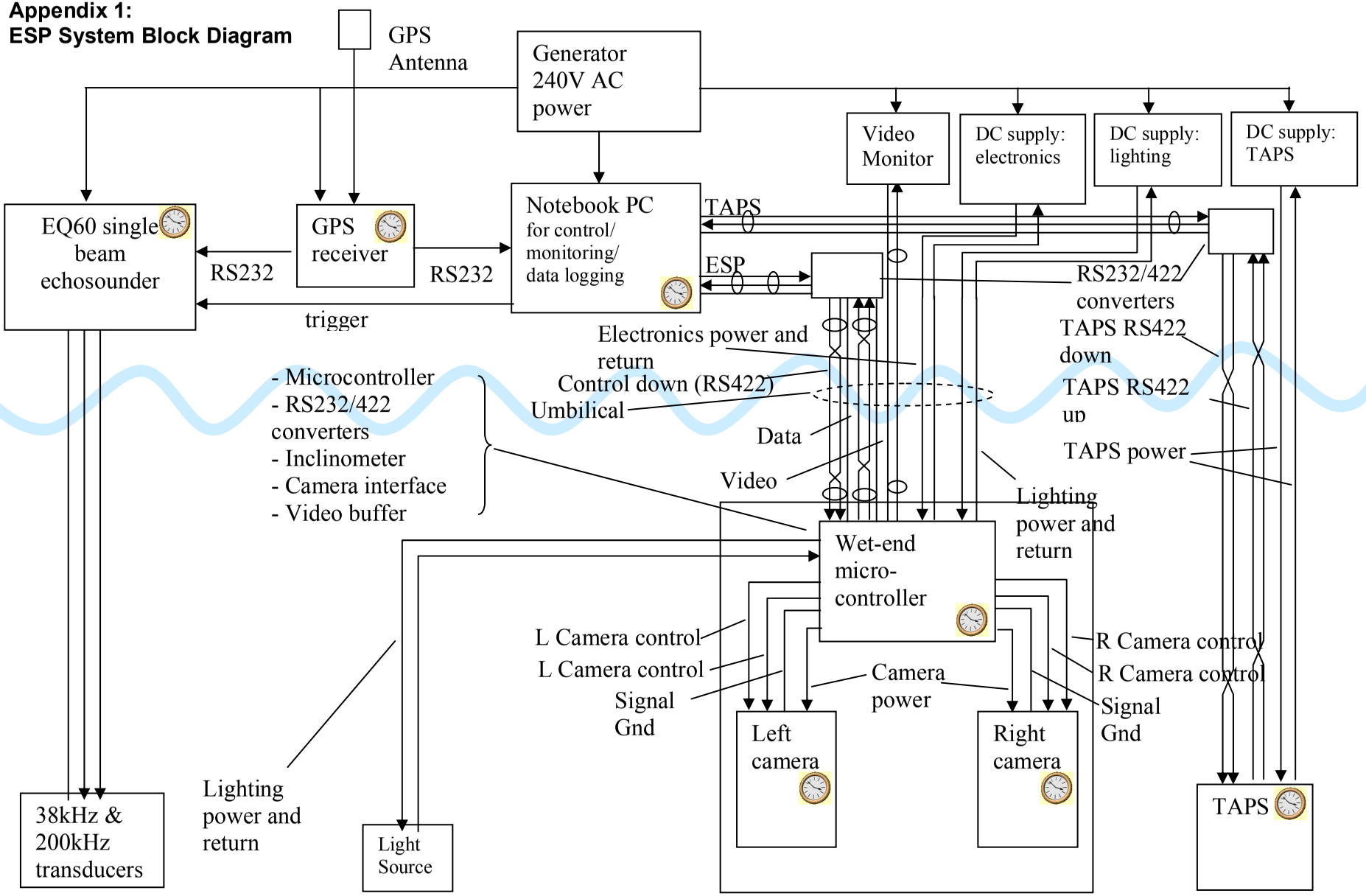

Appendix 2: Example Project Field Itinerary

EXAMPLE FIELD ITINERARY
COCKBURN SOUND, AUGUST 2004
ESP (Epibenthic Scattering Project)
COASTAL CRC, COASTAL WATER HABITAT MAPPING PROJECT

Last reviewed: 3 August 2004

Contacts:

Names and phone numbers (particularly mobile #) of all personnel (including shore based staff).

Personnel:

Full System Test: 4 staff
Davit installation: 1 staff
First Field Day: 4 staff

Equipment:

- ☐ Generator
- ☐ Fuel
- ☐ Extension cables
- ☐ Power board

- ☐ Deployment Rope
- ☐ Gloves
- ☐ Davit

- ☐ Cables:
- ☐ BX24 programming cable
- ☐ ESP umbilical
- ☐ ESP umbilical top end connector
- ☐ GPS to Splitter serial cable
- ☐ GPS splitter connector
- ☐ GPS Splitter to Acer#3 serial cable (DB9-DB9)
- ☐ GPS Splitter to EQ60 serial cable (DB9-DB9)
- ☐ EQ60 trigger cable (from laptop)

- ☐ Acer#3 (plus power supply, mouse, NI serial dongles)
- ☐ RS422 converter + power brick
- ☐ WEM to Acer serial cable (DB9-DB9)

- ☐ ESP Frame – including TAPS, Camera (WEM+Cameras), Light, EQ60
- ☐ Spare halogen bulb

- ☐ EQ60 computer and monitor (in ally road case)
- ☐ EQ60 transducer
- ☐ EQ60 power cable(s)

- ☐ TAPS (in frame)
- ☐ TAPS medium length underwater cable
- ☐ TAPS on/off plug

- ☐ TAPS interface box
- ☐ TAPS DB9 serial interface cable

- ☐ GPS unit (in ally road case)
- ☐ Antenna + coax cable
- ☐ GPS serial interface cable (DB9-DB25?)
- ☐ GPS power supply

- ☐ 2 x Battery Chargers
- ☐ USB CF card reader
- ☐ Canon 2MP digital still camera and bag

- ☐ Video camera
- ☐ Power supply
- ☐ Spare tapes
- ☐ Camera Video cable (RCA)
- ☐ BNC cables (+ extenders)
- ☐ BNC to RCA converters

- ☐ Field Toolkit
- ☐ Gaffa tape
- ☐ Covers/tarps

Personal Items:
- ☐ Sunscreen
- ☐ Wet weather gear
- ☐ Food + water

Procedures:

Day before:
Charge TAPS
Charge Camera Batteries

Evening Before:
Load all equipment into vehicle

First Field Day:
Transport boat to Cockburn Sound
6:30am arrive Cockburn sound
Setup equipment on boat
Launch boat

Perform simple test in shallow water to confirm operation of full system and deployment methods
Haul system to surface, remove memory cards, download images and check data.

Move to desired GPS location
Set Anchors
Deploy ESP
Acquire lots of data
Retrieve ESP

Move to next location (repeat above)

Demobilise equipment off boat
return boat to shed
return equipment to Curtin
wash down wet-end equipment

Appendix 3: Image Classification Classes used for the three field deployments

Image classification classes for 1st field trial, 10th August 2004

1st digit: species or classes	2nd digit: conditions
0 N/A	0 N/A
1 Sand	1 uniform
2 (originally assigned for gravel but never used)	2 non uniform
3 Bare Reef	3 Dense
4 Algae	4 sparse
5 P. sinuosa	5 attachment on seagrass
6 P. australis	6 Gas bubble appeared in the images
7 Mixture of 2 seagrasses	7 Coral
8 Fish appeared in images	8 macro algae
9 hard to tell from images	

%** Note: The '08' two digits combination is remained for muddy sand seafloor only.
%The '00' is remained for those images that were not able to be identified.
%YaoTing2005. This 2-digit is only for field trial on 2005 June 1 at
%Cockburn Sound.

Image classification classes for 2nd field trial, 1st June 2005

1st digit: species or classes	2nd digit: conditions
0 Not distinguishable	0 N/A
1 Sand	1 Sparse
2 Coral	2 Medium
3 Bare Reef	3 Dense
4 Algae	4 Non-homogeneous or non-uniform
5 P. sinuosa	5 Strange / unknown ?
6 P. australis	6 Gas bubble appeared in the images(not used)
7 Seagrass (but not sure the species)	7 Mix with other species, like sea squirts
8 Sea squirts	8 Mud (The second digit "8" is specifically reserved for mud only.)
9 Mussels	9

%** Note: The '08' two digits combination is remained for muddy sand seafloor only.
%The '00' is remained for those images that were not able to be identified.
%YaoTing2005. This 2-digit is only for field trial on 2005 June 1 at
%Cockburn Sound.

Image classification classes for 3rd field trial, 26th October 2005

1st digit: species or classes	2nd digit: conditions
0 Not distinguishable	0 N/A
1 Sand	1 Sparse
2	2 Medium
3	3 Dense or Pure
4	4 Non-homogeneous or non-uniform
5 Amphibolis griffithii	5 Strange ?
6 Amphibolis + Posidonia	6
7 Posidonia	7 Mix with other species, like sea squirts
8 Not recognized creatures	8
9	9

**Note:
The '00' is kept for those images that were not able to be identified.